

Detecting emergent continuous symmetries at quantum criticality

Mingru Yang,¹ Bram Vanhecke,¹ and Norbert Schuch^{1,2}

¹University of Vienna, Faculty of Physics, Boltzmannngasse 5, 1090 Wien, Austria

²University of Vienna, Faculty of Mathematics, Oskar-Morgenstern-Platz 1, 1090 Wien, Austria
(Dated: November 28, 2023)

New or enlarged symmetries can emerge at the low-energy spectrum of a Hamiltonian that does not possess the symmetries, if the symmetry breaking terms in the Hamiltonian are irrelevant under the renormalization group flow. In this letter, we propose a tensor network based algorithm to numerically extract lattice operator approximation of the emergent conserved currents from the ground state of any quantum spin chains, without the necessity to have prior knowledge about its low-energy effective field theory. Our results for the spin-1/2 J - Q Heisenberg chain and a one-dimensional version of the deconfined quantum critical points (DQCP) demonstrate the power of our method to obtain the emergent lattice Kac-Moody generators. It can also be viewed as a way to find the local integrals of motion of an integrable model and the local parent Hamiltonian of a critical gapless ground state.

Introduction.—Low-energy physics can show different symmetries from the Hamiltonian. In the thermodynamic limit, the continuous symmetry of a Hamiltonian can be spontaneously broken in its ground state, or new symmetries that the Hamiltonian does not possess can *emerge* in its low-energy spectrum. The latter phenomenon of emergent symmetries is prevalent at the critical point of many quantum and classical phase transitions, provided the symmetry breaking terms in the Hamiltonian are irrelevant under the renormalization group (RG) flow. The most prominent example might be the deconfined quantum critical point (DQCP) [1, 2], a direct continuous phase transition between two distinct spontaneous symmetry broken phases without fine-tuning, beyond the Landau-Ginzburg-Wilson paradigm. The emergent symmetry which reconciles the incompatible order parameters thus becomes the smoking gun to determine whether such a phase transition is really a DQCP. Another example is the extended symmetry in the low-energy eigenstates of a one-dimensional (1D) critical Hamiltonian with an internal semi-simple Lie group symmetry, when its low-energy physics is described by a conformal field theory (CFT) [3, 4]. In this case, the microscopic symmetry and the emergent symmetries can be recombined to form two independent symmetries acting respectively on the left- and right-moving fields, with the corresponding conserved charges being the zero modes of the Kac-Moody algebra [5, 6].

Plenty of numerical efforts [7–10] have been devoted to confirming the existence of emergent symmetries. In the case of DQCP, the identity between the scaling dimensions of the critical fluctuations related by emergent symmetries would be an indication [8, 11]. Other approaches include order parameter histograms [11, 12] and level-crossing analysis [13]. A more direct probe of emergent symmetries is to check if the scaling dimensions of the effective lattice operators for the conserved currents in the field theory are equal to the space dimension [8, 9]. However, identification of lattice operators to the currents in the continuum limit requires involved field theory and symmetry analysis [8, 14]. Moreover, the identification is

usually only approximate and also not unique.

Instead, tensor networks [15–18] provide us with much more information than simply a measurement outcome of the correlation function for given operators. In fact, rather than derive from field theory analysis, we are able to read out the lattice operator for the emergent conserved currents from a tensor network state in a straightforward way. Upon feeding a variationally optimized tensor network ground state [19, 20], our algorithm returns the optimal lattice approximation of the conserved current operators truncated to a given interaction range N , which systematically approximates the exact symmetry generators as N increases.

Algorithm.—If a state $|\psi\rangle$ is symmetric under a global continuous symmetry transformation $U = e^{i\epsilon O}$, then $U|\psi\rangle = e^{i\epsilon\phi}|\psi\rangle$. After absorbing the phase factor into the definition of O , i.e. $O \rightarrow O - \phi I$, we have $e^{i\epsilon O}|\psi\rangle = |\psi\rangle$, and its linearization gives

$$O|\psi\rangle = 0, \quad (1)$$

or $\langle\psi|O^\dagger O|\psi\rangle = 0$. For an internal symmetry with local generators, $O = \sum_n e^{ipn} G_{n,\dots,n+N-1}$, where p is the momentum and $G_{n,\dots,n+N-1}$ is a N -site operator starting at the n th site. Given a state $|\psi\rangle$ and a momentum p , if we aim to obtain an exact or approximate conserved quantity of this form which the state has, we can consider the optimization problem

$$\min_G f(G, G^\dagger) = \min_G \frac{\langle\psi|O^\dagger O|\psi\rangle}{V \text{Tr}[G^\dagger G]} \quad (2)$$

with the normalization constraint $\|G\|^2 = \text{Tr}[G^\dagger G] = 1$, where V is the system size. Note that this cost function has a physical interpretation of the static structure factor of G at momentum p . The unitarity of U requires O , and thus G , to be Hermitian. In that case, the optimum of f is reached when $\frac{\partial f}{\partial G} = 0$, i.e.

$$\langle\psi|\frac{\partial O^\dagger}{\partial G} O|\psi\rangle + \langle\psi|O^\dagger \frac{\partial O}{\partial G}|\psi\rangle = 2 \frac{\langle\psi|O^\dagger O|\psi\rangle}{\text{Tr}[G^2]} G, \quad (3)$$

which, after vectorizing $G \mapsto \mathbf{g}$, becomes an eigenvalue problem

$$(\mathcal{F} + \mathcal{F}^T) \cdot \mathbf{g} = 2\lambda_{min}\mathbf{g}, \quad (4)$$

where the eigenvalues are guaranteed to be non-negative real numbers due to the positive semi-definite quadratic form of the cost function f , and it can be proved [21] that the eigenvectors G are guaranteed to be Hermitian up to an arbitrary overall phase. For an eigenvector G , the associated eigenvalue λ naturally measures how accurate

the corresponding symmetry is.

For an infinite matrix product state (MPS) $|\psi\rangle$, this eigenvalue problem can be solved by adapting MPS techniques used in other contexts; readers not interested in these details can skip this paragraph. Take $|\psi\rangle$ as an infinite uniform MPS with one-site unit cell parameterized by tensors A_L , A_R , and A_C in the mixed gauge. The application of \mathcal{F} to \mathbf{g} , and similarly $\mathcal{F}^T \cdot \mathbf{g}$, can be implemented by observing that [22] it is the same as calculating the static structure factor of G except that a hole is dug in all the terms, i.e.

$$\begin{aligned} \mathcal{F} \cdot \mathbf{g} &= \langle \psi | \frac{\partial O^\dagger}{\partial G} O | \psi \rangle \\ &= \langle \psi | \left(\frac{1}{V} \sum_m e^{-ipm} \dots \left| \begin{array}{c} | \\ | \\ \dots \\ | \\ \dots \\ | \\ \dots \\ | \\ \dots \\ | \end{array} \right| \dots \right) \left(\sum_n e^{ipn} \dots \left| \begin{array}{c} | \\ \dots \\ | \\ \dots \\ | \\ \dots \\ | \\ \dots \\ | \end{array} \right| \dots \right) | \psi \rangle \\ &= e^{-ipN} \left(\text{Diagram 1} \right) + e^{ipN} \left(\text{Diagram 2} \right) + \dots + \left(\text{Diagram 3} \right) \end{aligned} \quad (5)$$

where the last “...” means sum over all diagrams with $1 \leq |n - m| \leq N - 2$, E_L^L and E_R^R are the left- and right-gauge MPS transfer matrices, and $(\cdot)^P$ denotes the pseudo-inverse resulting from the infinite geometric series [20] of all relative positions between G and the hole without overlap, which includes a regularization procedure effectively removing the disconnected part of the correlation functions and thus is automatically consistent with the phase factor absorption mentioned previously. We can then use an iterative eigensolver [23] to obtain the lowest several solutions [24].

In principle, the algorithm works for any MPS [25]. Particularly, we are interested in applying it to the variational uniform MPS (VUMPS) [19] approximation of the gapless ground state of 1D critical Hamiltonians. Since an MPS with finite bond dimension is always gapped [20], it can never exactly represent a critical ground state of infinite correlation length and thus can never exactly capture the symmetry of a critical lattice Hamiltonian or of its low-energy effective field theory in the infrared limit. However, we may use the principle of entanglement scaling [26–28] and treat the finite bond dimension χ as a

relevant perturbation, which enables us to identify the exact or emergent symmetries exclusively from the MPS through an extrapolation in the correlation length ξ , as shown by the benchmark results below.

Benchmarks for exact symmetries.—As a warming up, we first consider a critical model whose ground state has an exact $U(1)$ symmetry [29]—the spin-1/2 isotropic quantum XY chain

$$H = - \sum_n (X_n X_{n+1} + Y_n Y_{n+1}), \quad (6)$$

where X_n , Y_n , and Z_n are the Pauli matrices at site n . The $U(1)$ symmetry is generated by $O = \sum_n Z_n$ that satisfies $[H, \sum_n Z_n] = 0$. The model is integrable and thus has infinitely many local conserved quantities in the thermodynamic limit [30–33]. The critical low-energy physics is described [34] by the $U(1)_4$ CFT of free bosons with central charge $c = 1$.

Applying our algorithm to MPS of various bond dimensions yields the local conserved quantities up to $N = 3$. The full spectrum (after removing the trivial solutions) of the eigenvalue problem in Eq. (4) are shown in Fig. 1 and

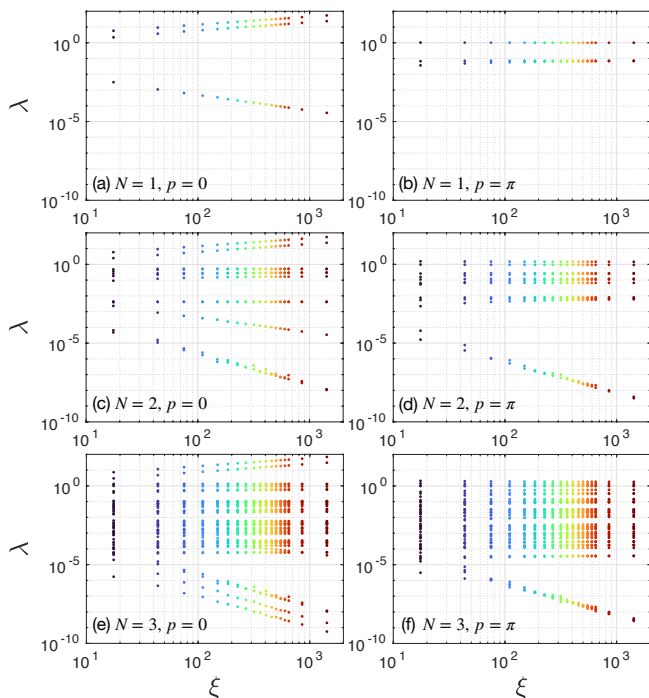


FIG. 1. Log-log plot of the eigenvalue spectrum of $\frac{1}{2}(\mathcal{F} + \mathcal{F}^T)$ versus the correlation length ξ for the spin-1/2 isotropic quantum XY chain. The correlation length of an MPS with a certain bond dimension is calculated by Eq. (40) in Ref. [20]. Notice that in (e) there is one decaying λ hidden in the bulk of larger eigenvalues but it becomes visible at larger correlation lengths.

the eigenvectors G associated with the decaying eigenvalues are shown in Table I. For $p = 0$, there are 1, 3, 5 eigenvalues decaying with the correlation length for $N = 1, 2, 3$, respectively; for $p = \pi$, there are 0, 2, 4 eigenvalues decaying with the correlation length for $N = 1, 2, 3$, respectively. The eigenvector $G = XX + YY$ corresponds to the Hamiltonian in Eq. (6), so as a by-product our method is also able to determine the local parent Hamiltonian [35–37] solely from its ground state. We notice that the decay has a power-law scaling $\lambda \sim \xi^{-\eta'}$ [38] and the exponents are listed in Table I. All other eigenvalues increase or stay constant with the increasing correlation length. The G 's associated with the decaying λ 's are local integrals of motion since λ is extrapolated to 0 at infinite correlation length. While the conserved quantities in Table I and more conserved quantities for larger N in the XY model can be constructed recursively [21] through the master symmetry approach [6, 30–32, 39], our method provides an alternative way to obtain them generally.

Extended symmetries by emergent symmetries.—The ground state of the spin-1/2 antiferromagnetic Heisenberg chain is expected to have an emergent symmetry in addition to the microscopic $SU(2)$ symmetry of the lattice Hamiltonian, and thus the symmetry is extended to $SO(4) = [SU(2)_L \times SU(2)_R]/\mathbb{Z}_2$ [5, 40]. Here, we consider

p	N	G	η'
0	1	Z	1.009
	2	$XX + YY$	1.985
	3	$XY - YX$	1.933
π	1	—	—
	2	$XX - YY$	2.005
	3	$XY + YX$	2.008
		$XZX - YZY$	2.046
		$XZY + YZX$	2.063

TABLE I. Local conserved quantities in the spin-1/2 isotropic quantum XY chain up to $N = 3$. Smaller- N solutions reappear at larger N and we only show the new solutions at each N . The η' is obtained from the scaling of $\langle \psi | O^\dagger O | \psi \rangle$ with ξ , which is slightly different from the slope of the decaying eigenvalues in Fig. 1, since different solutions can mix with each other and their form also become more accurate as ξ increases.

the J - Q model [7]—a modified Heisenberg chain at whose transition point still exists the extended symmetry—

$$H = -J \sum_n P_{n,n+1} - Q \sum_n P_{n,n+1} P_{n+2,n+3}, \quad (7)$$

where $P_{n,n+1} = 1/4 - \mathbf{S}_n \cdot \mathbf{S}_{n+1}$ with $\mathbf{S}_n = (S_n^x, S_n^y, S_n^z) = \frac{1}{2}(X_n, Y_n, Z_n)$. The dimer order enforced by strong four-site interaction transits to a critical phase when $Q/J \lesssim 0.84831$ [41, 42], at which [43] the effective description is the $c = 1$ $SU(2)_1$ Wess-Zumino-Witten (WZW) CFT [5, 40].

Fig. 2 shows the eigenvalues of our optimization problem after imposing the time reversal, parity, and spin flip symmetries [21] of the microscopic Hamiltonian at the transition point. The eigenvectors associated with all the eigenvalues shown in Fig. 2 except the faded ones are lattice operator approximation for the conserved currents of the extended symmetry to different precision, which could be confirmed by checking [21] that their scaling dimension is one [5]. To identify the eigenvalues that associate with the same G 's at different ξ , we search for the eigenvectors at smaller ξ 's which have the largest overlap with each of the lowest several eigenvectors at the largest ξ reached, as tracked by the colored lines in Fig. 2. The dots connected by blue and red lines at the bottom of the spectrum are the best approximation among all of the solutions. Different from the exact symmetries, eigenvalues corresponding to the emergent symmetries will finally saturate at some correlation length, because it is only a N -site truncated approximation of the exact emergent lattice generator.

We observe that three approximately conserved charges (red curves in Fig. 2), $M^\alpha = \sum_n m_n^\alpha$ ($\alpha \in \{x, y, z\}$), coming from the emergent symmetries, begin to appear at $N = 2$ in addition to the three exact microscopic $SU(2)$ symmetry generators (blue curves in Fig. 2) $Q^\alpha = \sum_n S_n^\alpha$, and they become more conserved as N

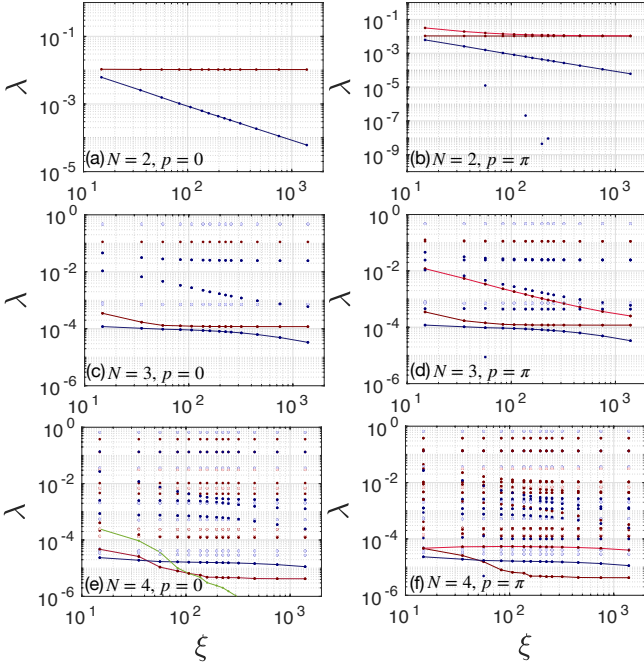


FIG. 2. Eigenvalue spectrum for the spin-1/2 J - Q Heisenberg model after imposing microscopic symmetries. The G 's associated with the blue (red) dots are parity even (odd) and time reversal odd (even). The scaling dimension of the G associated with the faded dots is not one and thus they are not emergent continuous internal symmetries. The green curve in (e) corresponds to the Hamiltonian. Notice that in (d)(f) one solution corresponding to one of the three generators for the exact $SU(2)$ symmetry of the microscopic Hamiltonian is not shown since it is well below 10^{-6} . We use a sublattice rotation about the z axis by angle π when using VUMPS to optimize the ground state, so the x and y components of the generators move to $p = \pi$.

increases, which is obvious from the drop of the corresponding eigenvalues. At $N = 2$, $m_{n,\alpha} = \epsilon_{\alpha\beta\gamma} S_n^\beta S_{n+1}^\gamma$ with $\epsilon_{\alpha\beta\gamma}$ the Levi-Civita symbol; at $N = 3$, next-nearest neighbor term shows up and we have $m_{n,\alpha} = \epsilon_{\alpha\beta\gamma} (w_1 S_n^\beta S_{n+1}^\gamma + w_2 S_n^\beta S_{n+2}^\gamma)$ with $w_2/w_1 \approx 0.2253$ [44]. The form of the 3-site $m_{n,\alpha}$ looks very similar to the level-1 Yangian [45–47]—which are exact conserved quantities of the RG fixed point, the Haldane-Shastry model [48, 49]—truncated to the next-nearest neighbor coupling, though with different coupling coefficients [21]. When going to $N = 4$, the contribution from longer-range coupling in the level-1 Yangian appears with all coupling coefficients modified. Moreover, terms from the level-3 Yangian begin to be involved. We get $m_{n,\alpha} = m_{n,\alpha}^1 + m_{n,\alpha}^3$, where $m_{n,\alpha}^1 = \epsilon_{\alpha\beta\gamma} (w_1 S_n^\beta S_{n+1}^\gamma + w_2 S_n^\beta S_{n+2}^\gamma + w_3 S_n^\beta S_{n+3}^\gamma)$ and $m_{n,\alpha}^3 = \epsilon_{\alpha\beta\gamma} [u_1 S_n^\beta S_{n+3}^\gamma \mathbf{S}_{n+1} \cdot \mathbf{S}_{n+2} + u_2 \mathbf{S}_n \cdot \mathbf{S}_{n+3} S_{n+1}^\beta S_{n+2}^\gamma + u_3 (S_n^\beta S_{n+1}^\gamma \mathbf{S}_{n+2} \cdot \mathbf{S}_{n+3} + \mathbf{S}_n \cdot \mathbf{S}_{n+1} S_{n+2}^\beta S_{n+3}^\gamma) + u_4 (S_n^\beta S_{n+2}^\gamma \mathbf{S}_{n+1} \cdot \mathbf{S}_{n+3} + \mathbf{S}_n \cdot \mathbf{S}_{n+2} S_{n+1}^\beta S_{n+3}^\gamma)]$, with $w_2/w_1 \approx 0.3557$, $w_3/w_1 \approx 0.1467$, $u_1/w_1 \approx 0.1577$, $u_2/w_1 \approx -0.09690$, $u_3/w_1 \approx -0.09141$, and $u_4/w_1 \approx 0.08169$. Considering that it is

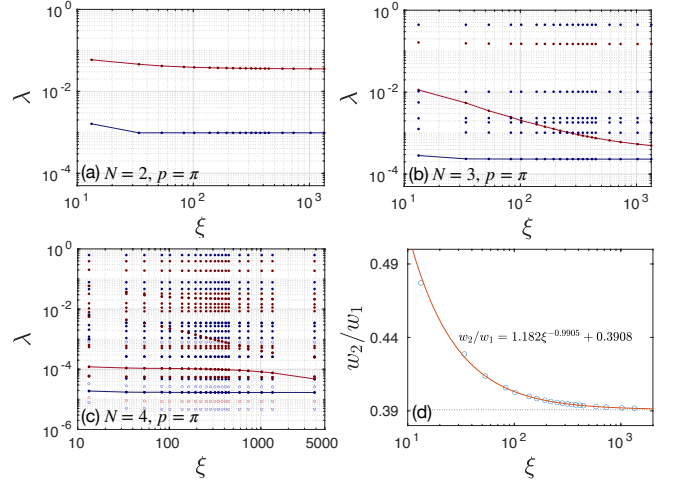


FIG. 3. Eigenvalue spectrum for the Jiang-Motrunich model after imposing microscopic symmetries at $p = \pi$ for (a) $N = 2$ (b) $N = 3$ (c) $N = 4$. The color convention is the same as in Fig. 2. (d) The ratio between the coefficient in front of the nearest neighbor term and next-nearest neighbor term in G_2 at $N = 3$ (the red curve in (b)).

even under time reversal and odd under parity, $M^\alpha \sim J_0^\alpha - \bar{J}_0^\alpha$, where J_0^α (\bar{J}_0^α) is the zero mode of the Kac-Moody generators, which form the ordinary Lie algebra $\mathfrak{su}(2)_L$ ($\mathfrak{su}(2)_R$) [50]. Since $Q^\alpha \sim J_0^\alpha + \bar{J}_0^\alpha$ [51], M^α and Q^α can then be linearly combined to construct J_0^α and \bar{J}_0^α , and other modes of the Kac-Moody generators can be constructed by the Fourier transform of the currents [6].

Emergent symmetries at a DQCP.—The following spin-1/2 chain, studied by Jiang and Motrunich [52],

$$H = \sum_n (-J_x X_n X_{n+1} - J_z Z_n Z_{n+1}) + \sum_n (K_{2x} X_n X_{n+2} + K_{2z} Z_n Z_{n+2}), \quad (8)$$

has an onsite $\mathbb{Z}_2 \times \mathbb{Z}_2$ spin-flip symmetry. It undergoes a direct continuous transition from a valence bond solid to ferromagnetic order at $K_{2x} = K_{2z} = 1/2$, $J_x = 1$, $J_z \approx 1.4645$ [8], which has been proposed to be a DQCP with an emergent $U(1) \times U(1)$ symmetry [8, 53] that is also generated by the zero modes of the Kac-Moody algebra.

Applying our algorithm to the critical point, we find a single solution $G = Z$ for $N = 1$. From $N = 2$, we require the eigenvectors to transform the same as Z under the spin flip symmetry when solving the eigenvalue problem, and find two solutions at $p = \pi$ as shown in Fig. 3(a,b,c). For $N = 2$, the lowest solution (blue) is $G_1 = ZI - IZ$ (i.e., a staggered Z), and the second solution (red) is $G_2 = XY + YX$, which satisfies $[G_1, G_2] = 0$; these are indeed precisely the same effective lattice operators identified as conserved currents for the emergent $U(1) \times U(1)$ symmetry through bosonization [8]. At $N = 3$, the corresponding eigenvalues for G_1 and G_2 improve by almost one and two orders of magnitude, respectively. The form of both solutions modifies

significantly by 3-site terms as compared to $N = 2$ —and thus compared to the field theory prediction— G_1 becomes $\frac{v_1}{3}(-ZII + IZI - IIZ) + v_2ZZZ + v_3(YYZ + ZYY) + v_4(XXZ + ZXX) + v_5XZX + v_6YZY$, with $v_2/v_1 \approx 0.1615$, $v_3/v_1 \approx 0.0988$, $v_4/v_1 \approx 0.0882$, $v_5/v_1 \approx 0.0410$, and $v_6/v_1 \approx -0.1399$; G_2 becomes $w_1[(XY+YX)I - I(XY+YX)] + 2w_2(XIY - YIX)$, with $w_2/w_1 \approx 0.3908$ (Fig. 3(d)). When pushing to $N = 4$, longer-ranged terms further dress G_1 and G_2 [21]. Our algorithm hence allows us to decorate upon the bare form of the lattice operators for emergent symmetry generators found through field theory analysis, and therefore to obtain a more precise picture of the microscopic nature of the emergent symmetries.

Conclusions.—We have presented a novel general method to numerically detect emergent continuous internal symmetries in critical systems. The bottom line is that emergent symmetries do not just reveal themselves indirectly in the long-distance behavior of correlation functions—which has been the sole detection mechanism before our work—but are actually realized surprisingly accurately on the lattice, albeit with spatially extended generators. We have illustrated this by rediscovering the theory-predicted lattice operators for the emergent conserved currents at a 1D DQCP and sharply improving them with newly discovered correction terms. We have also identified the effective lattice operators of the conserved charges for the extended $SO(4)$ symmetry in the J - Q chain with Yangian generators truncated to local terms, which were unknown before. The ability of our method to crack the explicit form of these lattice generators allows us to construct the emergent lattice Kac-Moody generators to unprecedented accuracy for both Abelian and non-Abelian symmetries [54] in generic settings.

Outlook.—This method could in principle be generalized to 2D, to extract emergent lattice conserved currents

in the projected entangled pair states (PEPS) [55–57], which would be of particular use for the study of higher-dimensional DQCP. A variant version with a larger unit cell can be easily derived. It is also worth exploring if a similar algorithm works for finite systems with periodic or other boundary conditions, for the low-energy excited states [58], or for classical systems. Adjusting this method to find unconventional symmetries of the weakly-entangled higher excited states [59, 60] or the emergent space-time symmetry [61] would be also interesting directions.

The complexity of the eigenvalue problem scales exponentially with N . To reduce the complexity of solving for G of larger size, we could resort to the density matrix renormalization group (DMRG) [15, 16] by treating G as an N -site finite matrix product operator (MPO) [62, 63], and the tricky part will be removing the trivial solutions efficiently [21, 24]. It would also be desirable to include terms with long-range tails by representing O as an infinite MPO [64], though its implementation encounters some technical difficulties [21].

Acknowledgments.—We thank Frank Verstraete, Natalia Chepiga, Jutho Haegeman, Laurens Vanderstraeten, Wen-Tao Xu, András Molnár, Anna Francuz, Ilya Kull, José Garre Rubio, Juraj Hasik, Rui-Zhen Huang, Pranay Patil, and especially Hong-Hao Tu for illuminating discussions. We also acknowledge the hospitality of the Erwin Schrödinger International Institute for Mathematics and Physics (ESI) during the long-term program “Tensor Networks: Mathematical Structures and Novel Algorithms”, which stimulated many of the discussions. This work has received support from the European Union’s Horizon 2020 program through Grant No. 863476 (ERC-CoG SEQUAM). The tensor contractions are implemented using `ncon` [65]. The codes are available on github [66].

-
- [1] T. Senthil, A. Vishwanath, L. Balents, S. Sachdev, and M. P. A. Fisher, Deconfined Quantum Critical Points, *Science* **303**, 1490 (2004).
 - [2] T. Senthil, L. Balents, S. Sachdev, A. Vishwanath, and M. P. A. Fisher, Quantum criticality beyond the Landau-Ginzburg-Wilson paradigm, *Phys. Rev. B* **70**, 144407 (2004).
 - [3] P. Francesco, P. Mathieu, and D. Sénéchal, *Conformal Field Theory* (Springer New York, NY, 1997).
 - [4] P. Ginsparg, *Applied Conformal Field Theory* (1991).
 - [5] I. Affleck, Critical Behavior of Two-Dimensional Systems with Continuous Symmetries, *Phys. Rev. Lett.* **55**, 1355 (1985).
 - [6] R. Wang, Y. Zou, and G. Vidal, Emergence of Kac-Moody symmetry in critical quantum spin chains, *Phys. Rev. B* **106**, 115111 (2022).
 - [7] P. Patil, E. Katz, and A. W. Sandvik, Numerical investigations of $SO(4)$ emergent extended symmetry in spin- $\frac{1}{2}$ Heisenberg antiferromagnetic chains, *Phys. Rev. B* **98**, 014414 (2018).
 - [8] R.-Z. Huang, D.-C. Lu, Y.-Z. You, Z. Y. Meng, and T. Xi-ang, Emergent symmetry and conserved current at a one-dimensional incarnation of deconfined quantum critical point, *Phys. Rev. B* **100**, 125137 (2019).
 - [9] N. Ma, Y.-Z. You, and Z. Y. Meng, Role of Noether’s Theorem at the Deconfined Quantum Critical Point, *Phys. Rev. Lett.* **122**, 175701 (2019).
 - [10] H. Dreyer, L. Vanderstraeten, J.-Y. Chen, R. Verresen, and N. Schuch, Robustness of critical $U(1)$ spin liquids and emergent symmetries in tensor networks (2020).
 - [11] A. W. Sandvik, Evidence for Deconfined Quantum Criticality in a Two-Dimensional Heisenberg Model with Four-Spin Interactions, *Phys. Rev. Lett.* **98**, 227202 (2007).
 - [12] J. Y. Lee, J. Ramette, M. A. Metlitski, V. Vuletic, W. W. Ho, and S. Choi, Landau-Forbidden Quantum Criticality in Rydberg Quantum Simulators (2022), arXiv:2207.08829 [cond-mat.str-el].

- [13] L. Wang and A. W. Sandvik, Critical Level Crossings and Gapless Spin Liquid in the Square-Lattice Spin-1/2 $J_1 - J_2$ Heisenberg Antiferromagnet, *Phys. Rev. Lett.* **121**, 107202 (2018).
- [14] M. Hermele, T. Senthil, and M. P. A. Fisher, Algebraic spin liquid as the mother of many competing orders, *Phys. Rev. B* **72**, 104404 (2005).
- [15] S. R. White, Density matrix formulation for quantum renormalization groups, *Phys. Rev. Lett.* **69**, 2863 (1992).
- [16] S. R. White, Density-matrix algorithms for quantum renormalization groups, *Phys. Rev. B* **48**, 10345 (1993).
- [17] R. Orús, Tensor networks for complex quantum systems, *Nature Reviews Physics* **1**, 538 (2019).
- [18] J. I. Cirac, D. Pérez-García, N. Schuch, and F. Verstraete, Matrix product states and projected entangled pair states: Concepts, symmetries, theorems, *Rev. Mod. Phys.* **93**, 045003 (2021).
- [19] V. Zauner-Stauber, L. Vanderstraeten, M. T. Fishman, F. Verstraete, and J. Haegeman, Variational optimization algorithms for uniform matrix product states, *Phys. Rev. B* **97**, 045145 (2018).
- [20] L. Vanderstraeten, J. Haegeman, and F. Verstraete, Tangent-space methods for uniform matrix product states, *SciPost Phys. Lect. Notes*, 7 (2019).
- [21] Supplementary material [URL will be inserted by publisher].
- [22] We adopt the same notation as in Ref. [20].
- [23] Y. Saad, *Numerical Methods for Large Eigenvalue Problems* (Society for Industrial and Applied Mathematics, 2011).
- [24] Notice that there always exist trivial solutions of the form $G = X \otimes I - I \otimes X$ for $p = 0$ and $G = X \otimes I + I \otimes X$ for $p = \pi$, with X being any $N - 1$ -site operator (except the identity) and I being the one-site identity. The N -site identity is also a trivial solution by regularization. The eigenvalues associated with those trivial solutions are exactly zero. In total they span a large trivial null space of dimension $d^{2(N-1)}$, where d is the dimension of the one-site physical Hilbert space. We have removed the trivial solutions from all of our results. Interested readers can go to the supplementary material [21] for how to remove the trivial solutions.
- [25] Solving the symmetry of the ground state of a gapped model is much easier, and another method based on the MPS fundamental theorem also works [21].
- [26] L. Tagliacozzo, T. R. de Oliveira, S. Iblisdir, and J. I. Latorre, Scaling of entanglement support for matrix product states, *Phys. Rev. B* **78**, 024410 (2008).
- [27] F. Pollmann, S. Mukerjee, A. M. Turner, and J. E. Moore, Theory of finite-entanglement scaling at one-dimensional quantum critical points, *Phys. Rev. Lett.* **102**, 255701 (2009).
- [28] M. M. Rams, P. Czarnik, and L. Cincio, Precise extrapolation of the correlation function asymptotics in uniform tensor network states with application to the Bose-Hubbard and XXZ models, *Phys. Rev. X* **8**, 041033 (2018).
- [29] In fact the symmetry should be $U(1) \times U(1)$. See Ref. [5].
- [30] E. Barouch and B. Fuchssteiner, Master symmetries and similarity equations of the XYh model, *Studies in Applied Mathematics* **73**, 221 (1985).
- [31] H. Araki, Master symmetries of the XY model, *Communications in Mathematical Physics* **132**, 155 (1990).
- [32] T. Matsui, On conservation laws of the XY model, in *Quantum and Non-Commutative Analysis: Past, Present and Future Perspectives*, edited by H. Araki, K. R. Ito, A. Kishimoto, and I. Ojima (Springer Netherlands, Dordrecht, 1993) pp. 197–204.
- [33] M. Fagotti, Local conservation laws in spin-1/2 XY chains with open boundary conditions, *Journal of Statistical Mechanics: Theory and Experiment* **2016**, 063105 (2016).
- [34] H.-H. Tu, Universal entropy of conformal critical theories on a Klein bottle, *Phys. Rev. Lett.* **119**, 261603 (2017).
- [35] J. R. Garrison and T. Grover, Does a single eigenstate encode the full hamiltonian?, *Phys. Rev. X* **8**, 021026 (2018).
- [36] X.-L. Qi and D. Ranard, Determining a local Hamiltonian from a single eigenstate, *Quantum* **3**, 159 (2019).
- [37] E. Chertkov and B. K. Clark, Computational Inverse Method for Constructing Spaces of Quantum Models from Wave Functions, *Phys. Rev. X* **8**, 031029 (2018).
- [38] Depending on the quantum number the operator carries, the correlation length of correlation functions of an operator can be different from the correlation length of the MPS [21]. It turns out that the critical exponents here have no universal relation to the scaling dimension of the corresponding operator [21].
- [39] K. Sogo and M. Wadati, Boost Operator and Its Application to Quantum Gelfand-Levitan Equation for Heisenberg-Ising Chain with Spin One-Half, *Progress of Theoretical Physics* **69**, 431 (1983).
- [40] I. Affleck and F. D. M. Haldane, Critical theory of quantum spin chains, *Phys. Rev. B* **36**, 5291 (1987).
- [41] Y. Tang and A. W. Sandvik, Method to characterize spinons as emergent elementary particles, *Phys. Rev. Lett.* **107**, 157201 (2011).
- [42] S. Sanyal, A. Banerjee, and K. Damle, Vacancy-induced spin texture in a one-dimensional $S = \frac{1}{2}$ Heisenberg antiferromagnet, *Phys. Rev. B* **84**, 235129 (2011).
- [43] The marginally irrelevant spin-umklapp term which introduces a logarithmic correction to the correlation function vanishes at the transition point, like in the J_1 - J_2 model [7, 48].
- [44] This form of the 3-site $m_{n,\alpha}$ and the ratio w_2/w_1 in the J - Q model is very similar to those in the J_1 - J_2 model [6]. They flow to the same RG fixed point and they are very similar even on the lattice level. To check this, we have performed exact diagonalization of a system size of 18 sites and found that the fidelity between their ground states is 0.9987.
- [45] F. D. M. Haldane, Z. N. C. Ha, J. C. Talstra, D. Bernard, and V. Pasquier, Yangian symmetry of integrable quantum chains with long-range interactions and a new description of states in conformal field theory, *Phys. Rev. Lett.* **69**, 2021 (1992).
- [46] J. C. Talstra and F. D. M. Haldane, Integrals of motion of the Haldane-Shastry model, *Journal of Physics A: Mathematical and General* **28**, 2369 (1995).
- [47] V. Drinfeld, Hopf algebras and the quantum Yang-Baxter equation, *Dokl. Akad. Nauk SSSR* **283**, 1060 (1985).
- [48] F. D. M. Haldane, Exact Jastrow-Gutzwiller resonating-valence-bond ground state of the spin- $\frac{1}{2}$ antiferromagnetic Heisenberg chain with $1/r^2$ exchange, *Phys. Rev. Lett.* **60**, 635 (1988).
- [49] B. S. Shastry, Exact solution of an $S = 1/2$ Heisenberg antiferromagnetic chain with long-ranged interactions

- tions, Phys. Rev. Lett. **60**, 639 (1988).
- [50] Notice that $J_\alpha + \bar{J}_\alpha$ also satisfies the $\mathfrak{su}(2)$ algebra, but $J_\alpha - \bar{J}_\alpha$ does not.
- [51] Strictly speaking, from bosonization [5] one knows that $S^\alpha(x) \sim (J_0^\alpha(x) + \bar{J}_0^\alpha(x)) + (-1)^x$ (term with scaling dimension $1/2$), however, the latter staggered part would cancel out upon sum over x and we get only $J_0^\alpha + \bar{J}_0^\alpha$.
- [52] S. Jiang and O. Motrunich, Ising ferromagnet to valence bond solid transition in a one-dimensional spin chain: Analogies to deconfined quantum critical points, Phys. Rev. B **99**, 075103 (2019).
- [53] B. Roberts, S. Jiang, and O. I. Motrunich, Deconfined quantum critical point in one dimension, Phys. Rev. B **99**, 165143 (2019).
- [54] Note that it happened to be easy to tell what the symmetry group the lattice generators obey in the above examples, had this not been the case we would have had to study the commutation relations of the generators projected onto the low-energy sector to discover the algebra.
- [55] F. Verstraete and J. I. Cirac, Renormalization algorithms for quantum-many body systems in two and higher dimensions (2004).
- [56] L. Vanderstraeten, M. Mariën, F. Verstraete, and J. Haegeman, Excitations and the tangent space of projected entangled-pair states, Phys. Rev. B **92**, 201111(R) (2015).
- [57] L. Vanderstraeten, J. Haegeman, and F. Verstraete, Simulating excitation spectra with projected entangled-pair states, Phys. Rev. B **99**, 165121 (2019).
- [58] J. Haegeman, B. Pirvu, D. J. Weir, J. I. Cirac, T. J. Osborne, H. Verschelde, and F. Verstraete, Variational matrix product ansatz for dispersion relations, Phys. Rev. B **85**, 100408(R) (2012).
- [59] M. Serbyn, Z. Papić, and D. A. Abanin, Local conservation laws and the structure of the many-body localized states, Phys. Rev. Lett. **111**, 127201 (2013).
- [60] S. Moudgalya and O. I. Motrunich, Numerical methods for detecting symmetries and commutant algebras, Phys. Rev. B **107**, 224312 (2023).
- [61] T.-C. Lin and J. McGreevy, Conformal field theory ground states as critical points of an entropy function (2023), arXiv:2303.05444 [hep-th].
- [62] G. M. Crosswhite and D. Bacon, Finite automata for caching in matrix product algorithms, Phys. Rev. A **78**, 012356 (2008).
- [63] G. M. Crosswhite, A. C. Doherty, and G. Vidal, Applying matrix product operators to model systems with long-range interactions, Phys. Rev. B **78**, 035116 (2008).
- [64] D. E. Parker, X. Cao, and M. P. Zaletel, Local matrix product operators: Canonical form, compression, and control theory, Phys. Rev. B **102**, 035147 (2020).
- [65] R. N. C. Pfeifer, G. Evenbly, S. Singh, and G. Vidal, Ncon: A tensor network contractor for matlab (2015), arXiv:1402.0939 [physics.comp-ph].
- [66] <https://github.com/mingruiyang/EmergentSymmetry>.

Supplementary material for “Detecting emergent continuous symmetries at quantum criticality”

CONTENTS

References	5
I. Imposing Hermiticity	i
II. Imposing microscopic symmetries	ii
III. Removing trivial solutions	iii
IV. Finite-system DMRG to optimize G	iv
V. The infinite uniform MPO formalism	iv
VI. Method based on the fundamental theorem of MPS	vi
VII. Conserved quantities in the spin-1/2 isotropic quantum XY chain	vii
VIII. Explanation of the critical exponents of the conserved quantities in the spin-1/2 isotropic quantum XY chain	vii
IX. More results of the spin-1/2 J - Q model	ix
X. Yangians in the Haldane-Shastry model	xii
XI. More results of the Jiang-Motrunich model	xii

I. IMPOSING HERMITICITY

In the main text, we mentioned that it can be proved that the eigenvectors G are guaranteed to be Hermitian up to an arbitrary overall phase. In the following, we will explain why this is true.

To make $U = e^{-i\epsilon O}$ unitary, O must be Hermitian. For $p = 0$ or $p = \pi$, G should also be Hermitian. Supposing G_n is a N -site Hermitian operator starting at site n , then

$$G_n = \sum_{\alpha=1}^{d^{2N}} c_{\alpha} v_{n,\alpha}, \quad (\text{S1})$$

where c_{α} is real and v_{α} is a N -site Kronecker product of the 1-site Hermitian basis operators $\{\frac{1}{\sqrt{2d}}I, T_1, \dots, T_{d^2-1}\}$, with d the dimension of the 1-site Hilbert space and T_i the $SU(d)$ generator in the fundamental representation.

Let's take $p = 0$ as an example. In this case, we have $O = \sum_n G_n$. The cost function will then become

$$f = \frac{\langle \psi | O^\dagger O | \psi \rangle}{V \text{Tr}[G^\dagger G]} = \frac{\sum_{n,m} \sum_{\alpha,\beta} c_{\alpha} c_{\beta} \langle \psi | v_{m,\beta} v_{n,\alpha} | \psi \rangle}{V \sum_{\alpha,\beta} c_{\alpha} c_{\beta} \text{Tr}(v_{\alpha} v_{\beta})} = \frac{2^N \sum_n \sum_{\alpha,\beta} c_{\alpha} c_{\beta} \langle \psi | v_{0,\beta} v_{n,\alpha} | \psi \rangle}{\sum_{\alpha} c_{\alpha}^2} = 2^N \frac{\mathbf{c}^T \cdot M \cdot \mathbf{c}}{\mathbf{c}^T \cdot \mathbf{c}}, \quad (\text{S2})$$

where we have used the fact that $\text{Tr}(v_{\alpha} v_{\beta}) = \frac{1}{2^N} \delta_{\alpha\beta}$ and translational invariance, with

$$M_{\beta\alpha} = \sum_n \langle \psi | v_{0,\beta} v_{n,\alpha} | \psi \rangle. \quad (\text{S3})$$

Then the first derivative becomes

$$\begin{aligned} \frac{\partial f}{\partial c_{\gamma}} &= 2^N \frac{(\sum_n \sum_{\beta} c_{\beta} \langle \psi | v_{0,\beta} v_{n,\gamma} | \psi \rangle) + \sum_n \sum_{\alpha} c_{\alpha} \langle \psi | v_{0,\gamma} v_{n,\alpha} | \psi \rangle}{(\sum_{\alpha} c_{\alpha}^2)^2} - \frac{(\sum_n \sum_{\alpha,\beta} c_{\alpha} c_{\beta} \langle \psi | v_{0,\beta} v_{n,\alpha} | \psi \rangle)(2c_{\gamma})}{(\sum_{\alpha} c_{\alpha}^2)^2} \\ &= 2^N \left[\frac{(\mathbf{c}^T \cdot M)_{\gamma} + (M \cdot \mathbf{c})_{\gamma}}{\mathbf{c}^T \cdot \mathbf{c}} - \frac{2(\mathbf{c}^T \cdot M \cdot \mathbf{c})c_{\gamma}}{(\mathbf{c}^T \cdot \mathbf{c})^2} \right]. \end{aligned} \quad (\text{S4})$$

If we let $\frac{\partial f}{\partial c_\gamma} = 0$, we will get

$$(\mathbf{c}^T \cdot M)_\gamma + (M \cdot \mathbf{c})_\gamma = \frac{2(\mathbf{c}^T \cdot M \cdot \mathbf{c})}{\mathbf{c}^T \cdot \mathbf{c}} c_\gamma, \quad (\text{S5})$$

or

$$[(M^T + M) \cdot \mathbf{c}]_\gamma = \frac{\mathbf{c}^T \cdot (M^T + M) \cdot \mathbf{c}}{\mathbf{c}^T \cdot \mathbf{c}} c_\gamma. \quad (\text{S6})$$

Therefore, in order to minimize f , we need to solve the eigenvalue problem

$$(M^T + M) \cdot \mathbf{c} = 2\tilde{\lambda}_{min} \mathbf{c} \quad (\text{S7})$$

with the constraint that \mathbf{c} is a real vector, which is automatically satisfied. This could be proved as the following. By utilizing translational invariance and the Hermiticity of $v_{n,\alpha}$, we can get that M is Hermitian, i.e.

$$M_{\alpha\beta}^* = \sum_n \langle \psi | v_{0,\alpha} v_{n,\beta} | \psi \rangle^* = \sum_n \langle \psi | v_{-n,\alpha} v_{0,\beta} | \psi \rangle^* = \sum_n \langle \psi | v_{n,\alpha} v_{0,\beta} | \psi \rangle^* = \sum_n \langle \psi | v_{0,\beta} v_{n,\alpha} | \psi \rangle = M_{\beta\alpha}. \quad (\text{S8})$$

So

$$M_{\alpha\beta}^* + M_{\beta\alpha}^* = M_{\beta\alpha} + M_{\alpha\beta}, \quad (\text{S9})$$

or

$$(M^T + M)^* = M + M^T, \quad (\text{S10})$$

i.e. $M^T + M$ is a real symmetric matrix, and hence it is guaranteed that it has real eigenvectors. Thus the G we obtain in this way will be automatically Hermitian operators.

Alternatively, we do not need to explicitly write G_n in the form of Eq. (S1) and solve the eigenvalues and eigenvectors of $M^T + M$. Instead, we could simply solve the eigenvalue problem of $\mathcal{F}^T + \mathcal{F}$, as stated in the main text, and its eigenvectors will be guaranteed to be Hermitian operators up to an arbitrary overall phase, which can be proved as follows. One could see that $M^T + M$ and $\mathcal{F}^T + \mathcal{F}$ are mapped to each other by

$$(M^T + M)_{\alpha\beta} = v_\alpha^T \cdot (\mathcal{F}^T + \mathcal{F}) \cdot v_\beta, \quad (\text{S11})$$

where v_α is a N -site Hermitian basis operator defined previously. Therefore, the eigenvalue problem of $M^T + M$ in Eq. (S7) is equivalent to

$$U^T (\mathcal{F}^T + \mathcal{F}) U \cdot \mathbf{c} = 2\tilde{\lambda}_{min} \mathbf{c} \quad (\text{S12})$$

or

$$(\mathcal{F}^T + \mathcal{F}) U \cdot \mathbf{c} = 2\lambda_{min} U \cdot \mathbf{c}, \quad (\text{S13})$$

where $\lambda_{min} = 2^N \tilde{\lambda}_{min}$ and $U = (v_1, \dots, v_{d^2N})$ is a basis transformation in the d^{2N} -dimensional complex space. Thus $U \cdot \mathbf{c}$ gives the G in Eq. (S1). Because \mathbf{c} is real and v_α is Hermitian, the eigenvectors of $\mathcal{F}^T + \mathcal{F}$ are guaranteed to be Hermitian.

II. IMPOSING MICROSCOPIC SYMMETRIES

Imposing the symmetries of the microscopic Hamiltonian will help to largely reduce the number of variational parameters and thus lower the complexity of the eigenvalue problem.

If the critical one-dimensional system is described by a CFT, the emergent conserved charges will be the zero modes of the Kac-Moody generators, J_0^α and \bar{J}_0^α . For $J_0^\alpha + \bar{J}_0^\alpha$, it would be time reversal odd and parity even; for $J_0^\alpha - \bar{J}_0^\alpha$, it would be time reversal even and parity odd. In addition, quantum spin Hamiltonians usually also have spin flip symmetries, and both J_0^α and \bar{J}_0^α will transform in the same way under the spin flip.

If we write G in the form of Eq. (S1) and solve the eigenvalue problem of $M^T + M$ to optimize \mathbf{c} , it will be easy to impose microscopic symmetries. For example, if $d = 2$, since $\mathcal{T}\vec{\sigma}\mathcal{T}^{-1} = -\vec{\sigma}$, to impose time-reversal symmetry, we can require the sum in Eq. (S1) to only include v_α with odd (even) number of Pauli matrices to make G odd (even)

under the time reversal; to impose parity symmetry, we can require the coefficients c_α to be $-c_\beta$ (c_β) if $v_\alpha \xrightarrow{\text{parity}} v_\beta$ to make G odd (even) under the parity transformation.

If we use the $\mathcal{F}^T + \mathcal{F}$ formalism, in principle we could restrict the entries in G similarly. But a more convenient way to impose microscopic symmetries when N is not large is to apply projection operators. For example, to make the eigenvector time-reversal even, one could solve the eigenvalue problem of $\mathcal{P}_+(\mathcal{F}^T + \mathcal{F})\mathcal{P}_+$ instead, where \mathcal{P}_+ is the projection operator onto the time-reversal even subspace. The operation $\mathcal{P}_+ \cdot \mathbf{x}$ could be implemented by mapping \mathbf{x} to $\mathbf{x} + \mathcal{T}\mathbf{x}$. In this way, all the time-reversal odd G will move to the null space. When N is not large, we can solve all the eigenvalues from the largest magnitude until we reach the null space and obtain the associated eigenvectors, and by the way we also exclude all the trivial solutions.

III. REMOVING TRIVIAL SOLUTIONS

As mentioned in footnote [24] of the main text, there is an issue to be remembered—the number of trivial solutions is large, i.e. $d^{2(N-1)}$, where d is the dimension of the local Hilbert space, so it would be desired to remove those trivial solutions.

It is easy to remove the trivial solutions in the $M^T + M$ formalism by restricting the operator strings v_α involved in Eq. (S1). We first need to exclude the N -site identity in Eq. (S1). To further avoid the $p = 0$ trivial solutions of the form $X \otimes I - I \otimes X$ (similarly for $p = \pi$), we can fix the coefficient in front of the term $X \otimes I$ and $I \otimes X$ in Eq. (S1) to be the same, without losing any generality, since it simply means that those terms can only appear as $N - 1$ site $G = X$ in a symmetric form in the N -site G .

In the $\mathcal{F}^T + \mathcal{F}$ formalism, as mentioned in the last section, when N is small, one could simply solve all the eigenvalues above the null space to exclude the trivial solutions. More generally, one could get rid of these trivial solutions by lifting those trivial solutions to the top of the spectrum, i.e. $\mathcal{F} \rightarrow \mathcal{F} + \alpha \mathcal{P}_{trivial}$, where a is some positive real number larger than λ_{max} of \mathcal{F} and $\mathcal{P}_{trivial}$ is the projection operator onto the trivial solution subspace. To obtain $\mathcal{P}_{trivial}$, we can consider the following problem to find the projection of a given operator G onto the trivial solution subspace, i.e.

$$\min_X \|G - (X \otimes I - I \otimes X)\|_2, \quad (\text{S14})$$

where $X \otimes I - I \otimes X$ is the form of the trivial solution at $p = 0$. By differentiating with respect to X , we get

$$X = \frac{1}{2d} \left(\left(\text{diagram 1} \right) - \left(\text{diagram 2} \right) + \left(\text{diagram 3} \right) + \left(\text{diagram 4} \right) \right), \quad (\text{S15})$$

which gives us a linear equation for X . If we map an operator X to a state $|X\rangle$, the above equation becomes

$$A|X\rangle = |b\rangle, \quad (\text{S16})$$

where

$$A = \left| \begin{array}{c} | \\ | \\ | \\ | \\ \dots \\ | \\ | \\ | \\ | \end{array} \right| - \frac{1}{2d} \left(\begin{array}{c} \text{diagram 5} \\ \text{diagram 6} \end{array} \right) \quad (\text{S17})$$

and

$$|X\rangle = \left(\text{diagram 7} \right) \quad (\text{S18})$$

and

$$|b\rangle = \frac{1}{2d} \left(\left(\text{diagram 8} \right) - \left(\text{diagram 9} \right) \right). \quad (\text{S19})$$

A has a null vector $|I\rangle$ since $A|I\rangle = 0$. But $I \otimes I - I \otimes I = 0$, so in the solution we can let the coefficient in front of the null vector to be zero without losing any generality. As a result, we get $|X\rangle = \text{pinv}(A)|b\rangle$, where $\text{pinv}(A)$ is the pseudo-inverse of A . Finally, the projection operator onto the trivial solution subspace should be

$$\mathcal{P}_{trivial} = \frac{1}{2d} \left(\left(\text{diagram 10} \right) + \left(\text{diagram 11} \right) - \left(\text{diagram 12} \right) - \left(\text{diagram 13} \right) \right). \quad (\text{S20})$$

Then we can perform $\mathcal{F} \rightarrow -(\mathcal{F} + \alpha \mathcal{P}_{trivial})$ to shift the trivial solution subspace to the top and reverse the spectrum so that the problem transforms to solving for the largest eigenvalues. $\mathcal{P}_{trivial}$ is model independent, so for each N we only need to solve for $\text{pinv}(A)$ once.

IV. FINITE-SYSTEM DMRG TO OPTIMIZE G

In the $\mathcal{F}^T + \mathcal{F}$ formalism, if we treat G as a single big tensor, the complexity of the optimization problem will grow exponentially as N increases. Alternatively, we can write G as a finite matrix product operator (MPO) and use the density matrix renormalization group (DMRG) [15, 16] to optimize it. Note that if we transform to the $M^T + M$ formalism, i.e. using the operator string v_α basis, the coefficient c_α can also be expressed as an MPO, and the advantage of using this basis is that the eigenvalue problem can be solved within real numbers.

Now let's take $N = 5$ as an example. A 5-site finite MPO is illustrated as

$$G = \begin{array}{c} | \\ \circlearrowleft W_1 \\ | \end{array} - \begin{array}{c} | \\ \circlearrowleft W_2 \\ | \end{array} - \begin{array}{c} | \\ \circlearrowleft W_3 \\ | \end{array} - \begin{array}{c} | \\ \circlearrowleft W_4 \\ | \end{array} - \begin{array}{c} | \\ \circlearrowleft W_5 \\ | \end{array}. \quad (\text{S21})$$

Different from treating G as a single big tensor, at each iteration we assume all but one site tensor W_i constant and differentiate the cost function f with respect to W_i only. If we let G in its canonical form, just like an MPS, we will get an eigenvalue problem for W_i at each iteration. We solve for the lowest eigenvalue at each iteration, and after several DMRG sweeps through the 5 sites we get a G corresponding to λ_{min} . Then we can construct a projection operator $\mathcal{P} = |G\rangle\langle G|$. Modifying the cost function to be $\mathcal{F} + \beta \mathcal{P}$ to lift this solution to the top of the spectrum, we perform the DMRG again to solve for the next solution.

Removing the large number of trivial solutions is essential for doing DMRG efficiently. In principle, we could do the same thing as in the last section. However, performing efficient DMRG requires us to have $\text{pinv}(A)$ either in the form of an MPO or decomposition of some local operators, while we currently do not have a good approach to efficiently calculate $\text{pinv}(A)$ when N becomes larger.

V. THE INFINITE UNIFORM MPO FORMALISM

A more natural representation for O , which is able to hold long-range interacting terms in the summation, would be the finite state automaton [62, 63], which can be translated to a infinite uniform MPO. This formalism also helps to reduce the complexity of the problem by solving for only one MPO site tensor and restricting the form of G to certain combination of Pauli strings. Here, we explain how to optimize a MPO for O of bond dimension $\chi_W = 2$, and show that the optimization for this MPO gives the same eigenvalue problem as in the main text. However, generalization from $\chi_W = 2$ to $\chi_W > 2$ is non-trivial and we leave it as an open question.

The MPO representation of O is

$$O = \dots - \begin{array}{c} | \\ \circlearrowleft W \\ | \end{array} - \begin{array}{c} | \\ \circlearrowleft W \\ | \end{array} - \begin{array}{c} | \\ \circlearrowleft W \\ | \end{array} - \begin{array}{c} | \\ \circlearrowleft W \\ | \end{array} - \begin{array}{c} | \\ \circlearrowleft W \\ | \end{array} - \dots, \quad (\text{S22})$$

where W is an operator-valued matrix given by

$$W = \begin{bmatrix} \mathbf{1} & G \\ 0 & \mathbf{1} \end{bmatrix}. \quad (\text{S23})$$

Then

$$\langle \psi | \frac{\partial O^\dagger}{\partial G^\dagger} O | \psi \rangle = \begin{array}{c} \left[\begin{array}{c} | \\ \circlearrowleft L^{[W]} \\ | \end{array} \right] \begin{array}{c} \circlearrowleft A_c \\ | \\ \circlearrowleft W \\ | \\ \circlearrowleft A_c \end{array} \left[\begin{array}{c} | \\ \circlearrowleft R^{[W]} \\ | \end{array} \right] \\ \hline \begin{array}{cc} 1 & 2 \end{array} \end{array} = D^{12,11} W_{11} + D^{12,12} W_{12} + D^{12,21} W_{21} + D^{12,22} W_{22} = D^{12,11} \mathbf{1} + D^{12,12} G + D^{12,22} \mathbf{1}. \quad (\text{S24})$$

Therefore we only need to calculate the fixed points $(L_{1,1}^{[\bar{W}W]}|, |R_{2,1}^{[\bar{W}W]})$, $(L_{1,2}^{[\bar{W}W]}|, |R_{2,2}^{[\bar{W}W]})$, which are defined as

$$(L_{a,b}^{[\bar{W}W]}| = \sum_{(a',b') \leq (a,b)} (L_{a',b'}^{[\bar{W}W]}|(T_L^{[\bar{W}W]})_{a',b';a,b}, \quad |R_{a,b}^{[\bar{W}W]} = \sum_{(a',b') \geq (a,b)} (T_R^{[\bar{W}W]})_{a,b;a',b'}|R_{a',b'}^{[\bar{W}W]}), \quad (\text{S25})$$

where

$$(T_{L/R}^{[\bar{W}W]})_{a',b';a,b} = \sum_{s,s',s''} \bar{A}_{L/R}^{s''} \otimes \bar{W}_{a',a}^{s',s''} \otimes W_{b',b}^{s,s'} \otimes A_{L/R}^s. \quad (\text{S26})$$

Notice that $\bar{W} \otimes W$ is still upper-triangular and there are two additional identities in the diagonal elements, i.e.

$$\bar{W} \otimes W = \begin{bmatrix} \mathbb{1} & G & G^\dagger & \mathbb{1} \\ 0 & \mathbb{1} & 0 & G^\dagger \\ 0 & 0 & \mathbb{1} & G \\ 0 & 0 & 0 & \mathbb{1} \end{bmatrix}. \quad (\text{S27})$$

From the definition, substituting the form of W , we get $(L_{1,1}^{[\bar{W}W]}| = (L_{1,1}^{[\bar{W}W]}|T_L$, where T_L is the transfer operator of the MPS $|\psi[A_L]\rangle$, so we have $(L_{1,1}^{[\bar{W}W]}| = |1\rangle$, where $|1\rangle$ is the left fixed point of T_L . We can then get $(L_{1,2}^{[\bar{W}W]}| = (L_{1,2}^{[\bar{W}W]}|T_L + (Y_{1,2}|$, where

$$(Y_{1,2}| = \begin{array}{c} \text{---} A_L \text{---} \\ | \\ \text{---} G \text{---} \\ | \\ \text{---} \bar{A}_L \text{---} \end{array}. \quad (\text{S28})$$

To remove the divergence from $\langle O \rangle$, one needs instead to solve the linear equation

$$(L_{1,2}^{[\bar{W}W]}|(1 - T_L + |R)(1) = (Y_{1,2}| - (Y_{1,2}|R)(1) \quad (\text{S29})$$

to get $(L_{1,2}^{[\bar{W}W]}|$. Similarly we can get $|R_{2,2}^{[\bar{W}W]} = |1\rangle$ and

$$(1 - T_R + |1)(L)|R_{2,1}^{[\bar{W}W]} = |Y_{2,1}\rangle - |1)(L|Y_{2,1}\rangle, \quad (\text{S30})$$

where

$$|Y_{2,1}\rangle = \begin{array}{c} \text{---} A_R \text{---} \\ | \\ \text{---} G \text{---} \\ | \\ \text{---} \bar{A}_R \text{---} \end{array}. \quad (\text{S31})$$

Therefore $D^{12,11}$ and $D^{12,22}$ are proportional to G and $D^{12,12}$ has no G dependence. It is easy to see that $D^{12,11}\mathbb{1} + D^{12,12}G + D^{12,22}\mathbb{1}$ is equivalent to $\mathcal{F} \cdot \mathbf{g}$ in the main text. If we require the normalization $\text{Tr}[G^\dagger G] = 1$, then we get the same eigenvalue problem as in the main text. So the $\chi_W = 2$ MPO formalism is equivalent to representing O as a summation of local terms in the case that G is one-site.

However, this equivalence could not be generalized to $\chi_W > 2$. For example, the most generic form for $\chi_W = 3$ is

$$W = \begin{bmatrix} \mathbb{1} & A & B \\ 0 & D & C \\ 0 & 0 & \mathbb{1} \end{bmatrix}. \quad (\text{S32})$$

If we want there to be some exponentially decaying interacting term, then $D = \kappa\mathbb{1}$ with $\kappa < 1$. There are several issues to optimize W . First, considering the simplest case with $D = 0$, the O generated by W would be $\sum_n (A_n C_{n+1} + B_n)$, and $\langle \psi|O^\dagger O|\psi \rangle$ contain terms linear in A , B , and C , so taking its derivative with respect to A , B , or C would not give us an eigenvalue problem, but one might be able to use the gradient descent method. The second question would be how to choose a proper normalization condition for W , especially when there is an exponentially decaying term. Simply requiring A , B , and C each to be individually normalized does not make sense. Probably the canonical form [64] for such Hamiltonian-like MPO might help.

VI. METHOD BASED ON THE FUNDAMENTAL THEOREM OF MPS

In footnote [25] of the main text, we mentioned that solving the symmetry of the ground state of a gapped system is much easier, and another method based on the MPS fundamental theorem also works. In this section, we will discuss this alternative method for gapped systems and why it does not work well for critical systems.

If an MPS

$$|\Psi(A)\rangle = \dots \text{---} \boxed{A} \text{---} \boxed{A} \text{---} \boxed{A} \text{---} \boxed{A} \text{---} \boxed{A} \text{---} \dots \quad (\text{S33})$$

is symmetric under a global on-site symmetry operation, the MPS tensor itself transforms under this operation [20]:

$$U_g^{\otimes N} |\Psi(A)\rangle \propto |\Psi(A)\rangle \quad \rightarrow \quad \text{---} \boxed{A} \text{---} = e^{i\phi_g} \text{---} \boxed{V_g} \text{---} \boxed{A} \text{---} \boxed{V_g^\dagger} \text{---} . \quad (\text{S34})$$

$\begin{array}{c} \text{---} \boxed{U_g} \text{---} \\ | \\ \text{---} \end{array}$

If the symmetry transformation is continuous, we can write $U_g = e^{ieG}$. After absorbing the phase factor $e^{i\phi_g}$ into the definition of G , the infinitesimal version becomes

$$\text{---} \boxed{A} \text{---} = \text{---} \boxed{1+ieK} \text{---} \boxed{A} \text{---} \boxed{1-ieK} \text{---} \quad (\text{S35})$$

$\begin{array}{c} \text{---} \boxed{1+ieG} \text{---} \\ | \\ \text{---} \end{array}$

or

$$\text{---} \boxed{A} \text{---} = \text{---} \boxed{K} \text{---} \boxed{A} \text{---} \text{---} \boxed{A} \text{---} \boxed{K} \text{---} . \quad (\text{S36})$$

$\begin{array}{c} \text{---} \boxed{G} \text{---} \\ | \\ \text{---} \end{array}$

After vectorizing $G \mapsto \mathbf{g}$ and $K \mapsto \mathbf{k}$, the above equation becomes

$$[P \quad Q - R] \begin{bmatrix} \mathbf{g} \\ \mathbf{k} \end{bmatrix} = 0, \quad (\text{S37})$$

where $P_{i\alpha\beta,jl} = \delta_{ij} A_{\alpha\beta}^l$, $Q_{i\alpha\beta,\gamma\rho} = \delta_{\rho\beta} A_{\alpha\gamma}^i$, and $R_{i\alpha\beta,\gamma\rho} = \delta_{\alpha\gamma} A_{\rho\beta}^i$. The equation can be transformed into a least square problem

$$\min_{\mathbf{x}} \|M \cdot \mathbf{x}\| \quad (\text{S38})$$

with constraint $\|\mathbf{x}\|_2 = 1$, where $M = [P \quad Q - R]$ and $\mathbf{x} = [\mathbf{g} \quad \mathbf{k}]^T$. This problem can be solved by either quadratic programming or singular value decomposition (SVD) $M = USV^\dagger$, where $S = \text{diag}(\lambda_1, \dots, \lambda_{d^2+D^2})$ and $V = (\mathbf{v}_1, \dots, \mathbf{v}_{d^2+D^2})$.

While it works for gapped systems, this way to solve for the symmetries is numerically unstable for the critical systems. In the benchmarks for the 1D isotropic XY model, it was observed that the singular vector \mathbf{v}_i whose first d^2 components best approximate the symmetry generator S_z does not always correspond to the second lowest singular value $\lambda_{d^2+D^2-1}$ (the trivial solution is the lowest one). In addition, the SVD only requires the orthogonality

$$[\mathbf{g} \quad \mathbf{k}]^\dagger \begin{bmatrix} \mathbf{g}' \\ \mathbf{k}' \end{bmatrix} = 0 \quad (\text{S39})$$

but not necessarily $\mathbf{g}^\dagger \mathbf{g}' = 0$, so there are many \mathbf{v}_j 's that have nonzero overlap with (S_z, K) . Also, we didn't see a clear scaling of the singular values with the correlation length.

Furthermore, M is not gauge invariant and so are its singular values. If we work in the mixed gauge, the infinitesimal version of the fundamental theorem becomes

$$\text{---} \boxed{A_C} \text{---} = \text{---} \boxed{K} \text{---} \boxed{A_R} \text{---} \text{---} \boxed{A_L} \text{---} \boxed{K} \text{---} \quad (\text{S40})$$

$\begin{array}{c} \text{---} \boxed{G} \text{---} \\ | \\ \text{---} \end{array}$

with $A_C = LAR$, $A_L = LAL^{-1}$, and $A_R = R^{-1}AR$. Notice that the trivial solution now becomes $(G, K) = (0, C)$, where $C = LR$. In the benchmarks for the 1D isotropic XY model, we could see a clear scaling of the singular values with the correlation length ξ . However, the problems are only partially solved by utilizing the mixed gauge. \mathbf{g} in the singular vectors is still not orthogonal to each other. As a result, we observed that the number of singular values that scales to zero with increasing correlation length is much larger than the number of symmetries the system actually has, though there is a gap between the lowest ones and the higher ones. The D^2 useless degrees of freedom for K also increase the complexity of the problem and make the solution quickly become unreachable as N and D increases. In addition, the singular values are not very physical, since they are still gauge dependent. In conclusion, for critical systems one should resort to the variational method in the main text.

Note that the on-site symmetry $\bigotimes_n U_g = \exp(-i\epsilon \sum_n G_n)$ can be generalized to a continuous symmetry $U = \exp(-i\epsilon O)$ generated by a summation of N -site local Hermitian operators $O = \sum_n G_{n, \dots, n+N-1}$, which takes a similar form to a local Hamiltonian. If the state is invariant under the transformation, i.e. $\exp(-i\epsilon O)|\psi\rangle = |\psi\rangle$ (the phase factor has been absorbed into the definition of O), it implies equivalently $O|\psi\rangle = \sum_n G_{n, \dots, n+N-1}|\psi\rangle = 0$, or

(S41)

for injective MPS, where G is a N -site operator and K is a $N-1$ -site tensor. Now there are $d^{2(N-1)}$ trivial solutions, which take the form $G = X \otimes I - I \otimes X$, where X is a $N-1$ -site operator and I is the one-site identity operator.

VII. CONSERVED QUANTITIES IN THE SPIN-1/2 ISOTROPIC QUANTUM XY CHAIN

In this section, we review the master symmetry [30] technique to obtain the conserved quantities in the spin-1/2 isotropic quantum XY chain.

The Hamiltonian of the spin-1/2 isotropic quantum XY chain can be written as

$$H = \sum_i h_i \quad (\text{S42})$$

where $h_i = X_i X_{i+1} + Y_i Y_{i+1}$. Obviously, H has a $U(1)$ symmetry and thus $[H, Q_0] = 0$, where $Q_0 = \sum_i Z_i$. Each term in the conserved quantity $Q_1 = \sum_i (X_i Y_{i+1} - Y_i X_{i+1})$ can be obtained by Eq. (46) in Ref. [6], i.e. $2i(X_i Y_{i+1} - Y_i X_{i+1}) = [h_i, Z_i]$. If we denote $H_0 = H$, each term in level- n conserved quantities $H_n = \sum_i h_{n,i}$ and $Q_n = \sum_i q_{n,i}$ can be constructed recursively up to a constant by

$$h_{n+1,i} \propto [h_i, H_n], \quad \text{if } n \geq 0; \quad (\text{S43a})$$

$$q_{n+1,i} \propto [h_i, Q_n], \quad \text{if } n \geq 1. \quad (\text{S43b})$$

For example, we have $H_1 = \sum_i (X_i Z_{i+1} Y_{i+2} - Y_i Z_{i+1} X_{i+2})$, and $Q_2 = \sum_i (X_i Z_{i+1} X_{i+2} + Y_i Z_{i+1} Y_{i+2})$. One can verify that

$$[H_n, H_m] = [H_n, Q_m] = [Q_n, Q_m] = 0. \quad (\text{S44})$$

For $p = \pi$ we could get in a similar way the conserved quantities that take a staggered pattern in the summation, $K = \sum_i (-1)^i k_i$.

VIII. EXPLANATION OF THE CRITICAL EXPONENTS OF THE CONSERVED QUANTITIES IN THE SPIN-1/2 ISOTROPIC QUANTUM XY CHAIN

For a correlation function $C(r, \xi) = \langle \psi | G_{n+r}^\dagger G_n | \psi \rangle$ near the critical point, it takes the form [28]

$$C(r, \xi) = r^{-\eta} g(r/\xi), \quad (\text{S45})$$

where $\eta = 2\Delta$ is double the scaling dimension of the operator G . Since the effect of finite bond dimension is like a relevant perturbation which deforms the MPS away from the exact critical point, the correlation function calculated

p	G	η'	η
0	Z	1.009	2
	$XX + YY$	1.985	2
	$XY - YX$	1.933	2
	$XZX + YZY$	1.008	2
	$XZY - YZX$	1.939	4
π	$XX - YY$	2.005	2
	$XY + YX$	2.008	2
	$XZX - YZY$	2.046	4
	$XZY + YZX$	2.063	4

TABLE I. The critical exponents η in the correlation function $C(r, \xi = \infty)$ and the critical exponent η' in $S(\xi) \sim \xi^{-\eta'}$ for the corresponding local conserved quantities in the spin-1/2 isotropic quantum XY chain up to $N = 3$. η is first obtained from calculating correlation functions analytically by Jordan-Wigner transformation and Wick's theorem and then further checked numerically.

with MPS should also take this form. In the continuum limit, the static structure factor S at momentum $p = 0$ is given by

$$S(\xi) = 2 \int_0^\infty dr r^{-\eta} g(r/\xi), \quad (\text{S46})$$

which should be invariant under a change of integration variable $x = \lambda r$, i.e.

$$S(\xi) = 2\lambda^{\eta-1} \int_0^\infty dx x^{-\eta} g(x/(\lambda\xi)) = \lambda^{\eta-1} S(\lambda\xi). \quad (\text{S47})$$

Therefore, we have $S(\lambda\xi) = \lambda^{-(\eta-1)} S(\xi)$, which yields

$$S(\xi) \sim \xi^{-(\eta-1)}, \quad (\text{S48})$$

i.e. the critical exponent for $S(\xi)$ is given by the critical exponent for the corresponding correlation function minus one, and to make $S(\xi)$ decay with increasing ξ it requires $\eta > 1$.

However, we find the above argument is oversimplified and thus does not generally hold. In TABLE I, one could observe that generally $\eta' \neq \eta - 1$ except for Z and $XZX + YZY$. Actually, the value of η' is extracted from calculation not in the continuum limit but within the discrete lattice, so

$$S(\xi) = 2 \sum_{r=1}^{\infty} C(r, \xi) + C(0, \xi). \quad (\text{S49})$$

For $XX + YY$ at $p = 0$, since $C(r, \xi = \infty) \sim (-1)^{r+1} r^{-2}$, for terms at large r the sum reduces to

$$\sum_r C(r, \xi) \sim \sum_{\text{odd } r} \left[\frac{1}{r^2} - \frac{1}{(r+1)^2} \right] = \sum_{\text{odd } r} \frac{1}{r^2} \left[1 - \left(1 + \frac{1}{r} \right)^{-2} \right] \approx \sum_{\text{odd } r} \frac{2}{r^3}. \quad (\text{S50})$$

Therefore effectively η becomes 3 and thus the relation $\eta' = \eta - 1$ still holds. For $XX - YY$ and $XY + YX$ at $p = \pi$, it could be argued similarly.

In fact, we found that η' depends on the behavior of the correlation function calculated with MPS not only in the infrared limit but at all distances. For a MPS, $C(r, \xi) \sim r^{-\eta} e^{-r/\xi}$ [28] is only true when r is much larger than the lattice spacing, and thus there is a certain range $\Lambda < r < \xi'$ where $C(r, \xi) \sim r^{-\eta}$. At short distance $r < \Lambda$, the behavior of $C(r, \xi)$ relies on microscopic details. At sufficiently large distance $r \gg \xi'$, we have $C(r, \xi) \sim e^{-r/\xi}$. As a result, weird cancellation can happen to give the final value of η' for $XZY - YZX$, $XZX - YZY$, and $XZY + YZX$, and it does not follow the previous simple argument.

Notice that the correlation length manifested in the correlation function calculated with MPS can be different from the correlation length obtained by the formula $\xi = -\frac{1}{\log|\lambda_2/\lambda_1|}$, where λ_i is the i th largest eigenvalue of the MPS transfer matrix $T = \sum_i \lambda_i |\lambda_i\rangle\langle\lambda_i|$. Define

$$(|G| = \text{Diagram}) \quad (\text{S51})$$

The reason is that $(G|\lambda_i)$ can be zero for the first several λ_i 's, depending on the charge G carries, and thus the correlation length will be instead given by $\xi = -\frac{1}{\log|\lambda_j/\lambda_1|}$, where λ_j is the largest eigenvalue of T that satisfies $(G|\lambda_j) \neq 0$. Nevertheless, we find that $\lambda_i = \lambda_2^{a_i}$ for $i > 2$, which will only bring a constant prefactor a_i to the correlation length and therefore will not affect the scaling.

IX. MORE RESULTS OF THE SPIN-1/2 J - Q MODEL

At the transition point $Q/J \approx 0.84831$, we first use VUMPS with 1-site unit cell to obtain the ground state for various bond dimensions from $\chi = 10$ to $\chi = 400$ until the gradient converges to 10^{-12} and then apply our algorithm to these uniform MPS. When doing VUMPS, we only require the MPS to be real so as to impose time-reversal symmetry but not impose any other microscopic symmetries. When applying our algorithm to the MPS obtained by VUMPS from $N = 2$, we impose the time-reversal, parity, and spin-flip symmetries as mentioned in the previous section. Since the one-site unit cell enforces translational invariance, we would get a (non-injective) equal weight superposition of all translational symmetry broken MPS ground state approximation, if it energetically favors a translational symmetry broken ground state within finite bond dimension, and thus it would limit the precision VUMPS can reach [19]. To avoid this, we perform a sublattice spin rotation around the z -axis by angle π when doing VUMPS, which is important for it to converge. Due to this sublattice rotation, the x and y components of the generators move to $p = \pi$.

As a supplemental, here we also show the data for $N = 1$, where we obtain the three generators for the microscopic SU(2) symmetry. For $p = 0$, we get only one decaying solution, $G = Z$ (blue curve in Fig. S1(a)); for $p = \pi$, we get two decaying solutions corresponding to the other microscopic SU(2) generators X and Y (blue curve and scattered points below it in Fig. S1(b)). Notice that most of those scattered points are well below 10^{-8} and not shown.

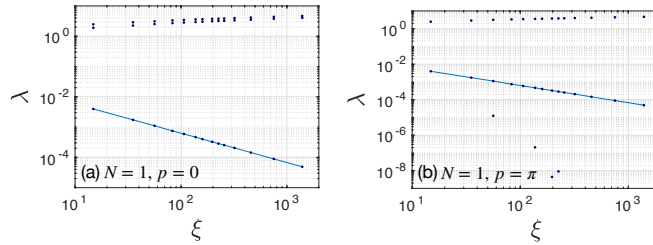


FIG. S1. Log-log plots of the non-trivial eigenvalue spectrum (without imposing microscopic symmetries) of \mathcal{F} versus the correlation length ξ for the spin-1/2 J - Q chain at $Q/J \approx 0.84831$ when $N = 1$.

The conservation of currents in 1 + 1d implies their scaling dimension must be 1 [5], which means their correlation functions should decay as r^{-2} . This is indeed the case as shown in Fig. S2, which plots the correlation function of q_z and m_z for different N , where $Q_z = \sum_x q_z(x)$ and $M_z = \sum_x m_z(x)$ are the zero modes of the Kac-Moody generators. We can see that

$$\langle q_z(0)q_z(r) \rangle \sim c_1(-1)^r r^{-1} + c_2 r^{-2}, \quad \langle m_z(0)m_z(r) \rangle \sim r^{-2}. \quad (\text{S52})$$

Notice that $\langle q_z(0)q_z(r) \rangle \sim r^{-2}$ for even N because of the cancellation of the staggered part due to terms like $G \otimes I + I \otimes G$, where G is a $N - 1$ -site operator, as listed in Table II. This cancellation can be explained as follows. If $\langle G(0)G(r) \rangle \sim c_1(-1)^r r^{-1} + c_2 r^{-2}$, then

$$\begin{aligned} & \langle (G \otimes I + I \otimes G)(0)(G \otimes I + I \otimes G)(r) \rangle \\ &= \langle G(0)G(r) \rangle + \langle G(0)G(r+1) \rangle + \langle G(1)G(r) \rangle + \langle G(1)G(r+1) \rangle \\ &= 2[c_1(-1)^r r^{-1} + c_2 r^{-2}] + c_1(-1)^{r+1}(r+1)^{-1} + c_2(r+1)^{-2} + c_1(-1)^{r-1}(r-1)^{-1} + c_2(r-1)^{-2} \\ &\sim 4c_2 r^{-2}. \end{aligned} \quad (\text{S53})$$

Note that although for q_α at $N > 2$ we got longer-range decoration to the 1-site spin operator S_α from terms in higher even-level Yangian generators. Those decorations will finally vanish as the correlation length goes to infinity, as shown in Fig. S3.

In Fig. S4 we also show the extrapolation of the coefficient ratio in m_z for $N = 4$.

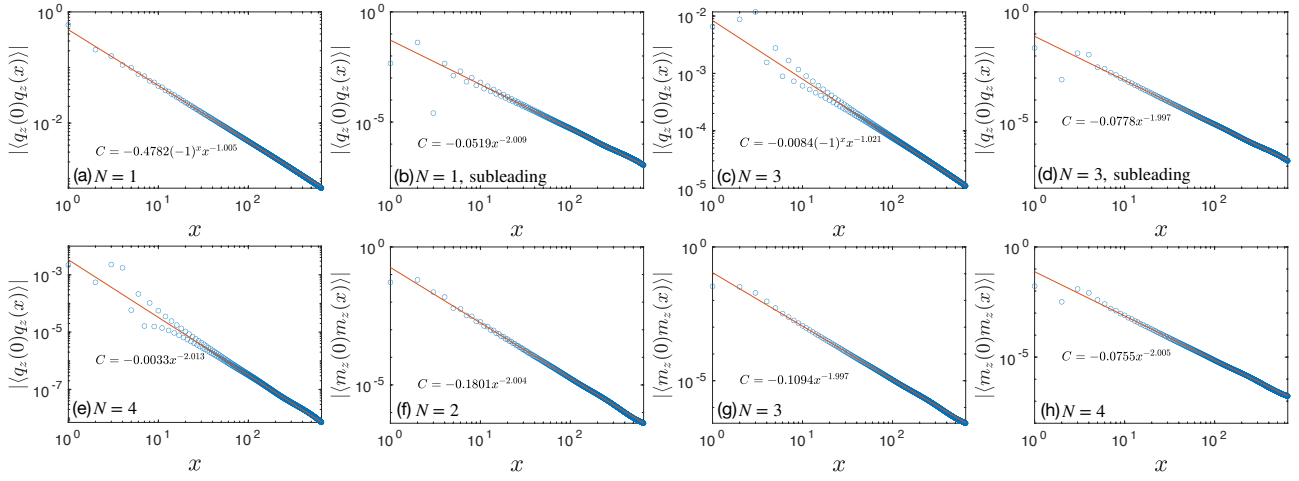


FIG. S2. The absolute value of the correlation function $\langle q_z(0)q_z(x) \rangle$ and $\langle m_z(0)m_z(x) \rangle$ measured with MPS of bond dimension $\chi = 240$, where q_z and m_z are the optimized solution for MPS of bond dimension $\chi = 400$. The subleading part of the correlation function of the N -site operator G is obtained by measuring the correlation function of $G \otimes I + I \otimes G$, and therefore the subleading part of the correlation function of the 1-site q_z is equivalent to the correlation function of the 2-site q_z .

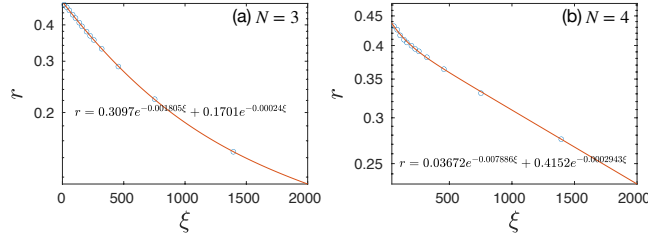


FIG. S3. (a) The weight of the part excluding S^z in q_z for (a) $N = 3$ and (b) $N = 4$ versus the correlation length ξ .

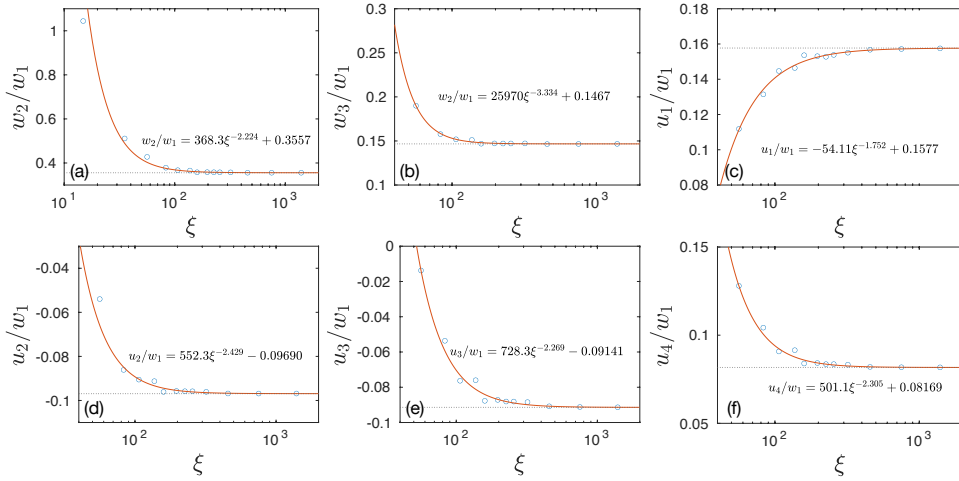


FIG. S4. (a) The ratio between the coefficients of the terms in m_z for $N = 4$ versus ξ , similarly for m_x and m_y .

p	N	\mathcal{P}	\mathcal{T}	G
0	1	+	-	Z
	2	+	-	$ZI + IZ$
		-	+	$XY - YX$
	3	+	-	$0.201918(ZII + IZI + IIZ)$ $-0.016479(XXZ + ZXZ + YYZ + ZYY) - 0.028084(XZX + YZY) + 0.004873ZZZ$
		-	+	$0.168431[(XY - YX)I + I(XY - YX)] - 0.075906(XIY - YIX)$
	4	+	-	$0.120163(III + IZI + IZII + ZIII)$ $+0.020134(ZIZZ + ZZIZ) + 0.019189(IZZZ + ZZZI)$ $-0.015721(IXXZ + IZXZ + XXZI + ZXZI + IYYZ + IZYY + YYZI + ZYYI)$ $-0.012254(IXZX + XZXI + IYZY + YZYI)$ $+0.009580(XIXZ + ZXIX) + 0.009581(YIYZ + ZYIY) - 0.007155(XXIZ + ZIXX) - 0.007156(YYIZ + ZIYY)$ $-0.003398(XIZX + XZIX) - 0.003397(YIZY + YZII)$
		-	+	$0.090323(-IIXY + IIXX - IXZI + IYZI - XYII + YXII)$ $+0.048202(IXIY - IYIX + XIYI - YIXI) - 0.039748(XIYY - YIIX)$
				$-0.010666(XZZY - YZZX) + 0.010015(XXXY - YXXZ) + 0.010014(XYYY - YYYX)$ $+0.006560(ZXYZ - ZYXZ) + 0.005165(XXYX - YYXY - XYXX + YXYY)$ $+0.006189(XYZZ - ZZYX) - 0.006190(YXZZ - ZZXY)$ $+0.005537(XZYZ - ZYZX) - 0.005536(YZXX - ZXZY)$
		+	+	$0.0761[II(XX + YY - ZZ) + I(XX + YY - ZZ)I + (XX + YY - ZZ)II]$ $+0.034(XX + YY - ZZ)(XX + YY - ZZ)$
	π	1	+	-
2		+	-	$0.242768(IX - XI) + (IY - YI)$
		-	+	$(IX - XI) - 0.242768(IY - YI)$ $0.242768(XZ + ZX) + (YZ + ZY)$ $(XZ + ZX) - 0.242768(YZ + ZY)$
3		+	-	$0.242768(XII - IXI + IIX) + (YII - IYI + IYY)$ $+0.139087(XYX + ZYZ) - 0.081610(XXY + YXX - YZZ - ZZY)$ $+0.033766(YXY + ZXZ) - 0.019812(XYY + YYX - XZZ - ZZX)$ $-0.024133YYY - 0.005859XXX$
		-	+	$(XII - IXI + IIX) - 0.242768(YII - IYI + IYY)$
				$0.242768[I(XZ + ZX) - (XZ + ZX)I] - 0.109859(XIZ - ZIX)$ $[I(YZ + ZY) - (YZ + ZY)I] - 0.452528(YIZ - ZIY)$ $[I(XZ + ZX) - (XZ + ZX)I] - 0.450663(XIZ - ZIX)$ $-0.242768[I(YZ + ZY) - (YZ + ZY)I] + 0.109407(YIZ - ZIY)$ $-0.007000(XXZ - ZXZ) - 0.007346(YYZ - ZYY)$
		+	-	$0.242768(III - IIXI + IXII - XIII) + (IIY - IYYI + IYII - YIII)$ $+0.167554(YIYY - YYIY) + 0.159692(YYYY - IYYY)$ $+0.130831(YXXI - IXXY + XXYI - IYXX) + 0.130834(IYZZ - ZZYI + IZZY - YZZI)$ $+0.101976(IXYX - XYXI + IYZZ - ZYZI) + 0.079728(XIXY - YXIX) - 0.079730(YZIZ - ZIZY)$ $-0.059546(XXIY - YIXX) - 0.059552(YIZZ - ZZII)$ $+0.040675(XIXX - XZIX) - 0.038766(IXXX - XXXI)$ $+0.031763(-IXYY + XYYI + YXYI - IYYX) + 0.031762(IXZZ - XZZI - ZZZI + IZZX)$ $+0.028275(XIYX - XYIX) - 0.028272(ZIYZ - ZYIZ)$ $+0.024755(IYXY - YXYI) + 0.024756(IZXZ - ZXZI)$ $-0.019357(XYIY - YIYX) - 0.019356(XZIZ - ZIZX)$ $+0.014457(XIYY - YYIX - XIZZ + ZZIX) - 0.006866(YXII - YIXY) - 0.006863(ZIXZ - ZXIZ)$
+		-	$(III - IIXI + IXII - XIII) - 0.242768(IIY - IYYI + IYII - YIII)$	
4		-	+	$0.242768(IIXZ - IXZI + XZII + IIZX - IZXI + ZXII)$ $-0.251227(IXIZ - XIZI - IZIX + ZIXI) + 0.271729(XIIZ + ZIIX)$ $+ (IIZZ - IYZI + YZII + IIZY - IZYI + ZYII)$ $-1.034842(IYIZ - YIZI - IZII + ZIYI) + 1.119294(YIIZ + ZIYY)$ $-0.501097(YYYZ + ZYYZ) + 0.501096(YZZZ + ZZZZ)$ $-0.256485(XYXZ + ZXYX - XZXY - YXZX)$ $-0.233853(XXYZ + ZYXX) - 0.233854(XXZY + YZXX)$ $-0.121652(XXXZ + ZXXZ) + 0.121650(XZZZ + ZZZX)$ $+0.107080(YYZY + YZYX - ZYZZ - ZZZZ)$ $+0.084445(XYZX + XZYX) + 0.062267(XYZY + YZYX) - 0.062265(ZYXY + YXYZ)$ $-0.056771(XZYY + YYZZ + YYZX + ZXYX)$ $-0.025996(ZXZZ + ZZXZ) + 0.025995(XXZX + XZXX)$ $+0.20501(YXZY + YZXY) - 0.010763(YXXZ + ZXXY)$
				$IIXZ - IXZI + XZII + IIZX - IZXI + ZXII$
	-	+	$-0.533663(IXIZ + ZIXI - IZIX - XIZI) + 0.440072(XIIZ + ZIIX)$ $-0.242768(IYZZ - IYZI + YZII + IIZY - IZYI + ZYII)$ $+0.129556(IYIZ + ZIYI - IZII - YIZI) - 0.106835(YIIZ + ZIYY)$ $-0.110877(XXXZ + ZXXX) - 0.118095(XYYZ + ZYYX) + 0.110874(XZZZ + ZZZX)$ $-0.072633(YXZY + YZXY) + 0.057187(XXZX + XZXX) - 0.057189(ZXZZ + ZZZZ)$ $+0.068534(YYXZ + ZXYX) + 0.068521(XZYX + YZYX) + 0.061302(XYZY + YZYX) - 0.061288(YXYZ + ZYXY)$ $+0.028678(YXXZ + ZXXZ) + 0.026910(YYYZ + ZYYZ) - 0.026917(YZZZ + ZZZZ)$ $+0.017634(XYZX + XZYX) - 0.016634(XXYZ + ZYXX) - 0.016630(XXYZ + ZYXX)$ $+0.014886(XYXZ + ZXYX) - 0.014881(XZXY + YXZX) - 0.013884(YYZY + YZYX - ZYZZ - ZZZZ)$	
			$-0.533663(IXIZ + ZIXI - IZIX - XIZI) + 0.440072(XIIZ + ZIIX)$ $-0.242768(IYZZ - IYZI + YZII + IIZY - IZYI + ZYII)$ $+0.129556(IYIZ + ZIYI - IZII - YIZI) - 0.106835(YIIZ + ZIYY)$ $-0.110877(XXXZ + ZXXX) - 0.118095(XYYZ + ZYYX) + 0.110874(XZZZ + ZZZX)$ $-0.072633(YXZY + YZXY) + 0.057187(XXZX + XZXX) - 0.057189(ZXZZ + ZZZZ)$ $+0.068534(YYXZ + ZXYX) + 0.068521(XZYX + YZYX) + 0.061302(XYZY + YZYX) - 0.061288(YXYZ + ZYXY)$ $+0.028678(YXXZ + ZXXZ) + 0.026910(YYYZ + ZYYZ) - 0.026917(YZZZ + ZZZZ)$ $+0.017634(XYZX + XZYX) - 0.016634(XXYZ + ZYXX) - 0.016630(XXYZ + ZYXX)$ $+0.014886(XYXZ + ZXYX) - 0.014881(XZXY + YXZX) - 0.013884(YYZY + YZYX - ZYZZ - ZZZZ)$	

TABLE II. Optimal lattice operator approximation of the conserved currents for the extended symmetry in the spin-1/2 J - Q chain at $Q/J \approx 0.84831$ up to $N = 4$ with $\chi = 400$. There are 3 generators associated to the exact microscopic $SU(2)$ symmetry and the corresponding eigenvalues of \mathcal{F} decays in a power law with the correlation length ξ : Z has $\eta' \approx 1.027$, while $0.242768X + Y$ and $X - 0.242768Y$ have $\eta' \approx 1.028$. Notice the effect on the signs from the sublattice rotation. And also notice that different (approximate) symmetry generators can be linearly combined with each other to form an eigenvector. $+$ ($-$) means parity \mathcal{P} or time reversal \mathcal{T} even (odd).

X. YANGIANS IN THE HALDANE-SHASTRY MODEL

In the last section, we mentioned that the lattice form of the Kac-Moody generators in the J - Q model looks like local truncation to the Yangian generators, which are exact symmetry of the Haldane-Shastry model. In this section, we give the explicit lattice forms of the Yangian generators up to level 3.

Yangian is a Hopf algebra and its level- n generators can be defined recursively starting from the level-0 and level-1 generators [47]. For $SU(2)$, the level-0 generators are the usual global $SU(2)$ generators, i.e. $Q_0^\alpha = \sum_i S_i^\alpha$. The level-1 generators are

$$Q_1^\alpha = \frac{1}{2} \sum_{i \neq j} w_{ij} i \epsilon^{\alpha\beta\gamma} S_i^\beta S_j^\gamma \quad (\text{S54})$$

with $w_{ij} = (z_i + z_j)/(z_i - z_j)$ and $z_j = \exp(2\pi i j/L)$, where L is the size of the system with periodic boundary condition. By utilizing the recursive relation

$$i \epsilon^{\alpha\beta\gamma} [Q_1^\gamma, Q_{n-1}^\beta] = 2Q_n^\alpha, \quad (\text{S55})$$

it can be derived that

$$Q_2^\alpha = \frac{1}{12} (N-1)(N-2)Q_0^\alpha - \sum_{i \neq j \neq k} w_{ij} w_{kj} S_i^\alpha \mathbf{S}_j \cdot \mathbf{S}_k \quad (\text{S56})$$

and

$$Q_3^\alpha = \frac{1}{6} (N-1)(N-2)Q_1^\alpha + \frac{1}{2} \sum_{i \neq j \neq l \neq m} w_{li} (w_{ml} - w_{mi}) (w_{jl} - w_{ji}) i \epsilon^{\alpha\beta\gamma} S_i^\beta S_j^\gamma \mathbf{S}_l \cdot \mathbf{S}_m. \quad (\text{S57})$$

We could see that the odd (even) level Yangian generators are odd (even) under the parity transformation.

XI. MORE RESULTS OF THE JIANG-MOTRUNICH MODEL

At $K_{2x} = K_{2z} = 1/2$, $J_x = 1$, $J_z \approx 1.4645$, we perform VUMPS [22] with 1-site unit cell from bond dimension $\chi = 10$ to $\chi = 400$ until the gradient converges to 10^{-12} and then apply our algorithm. We also tried two-site unit cell but did not see a notable difference in the results.

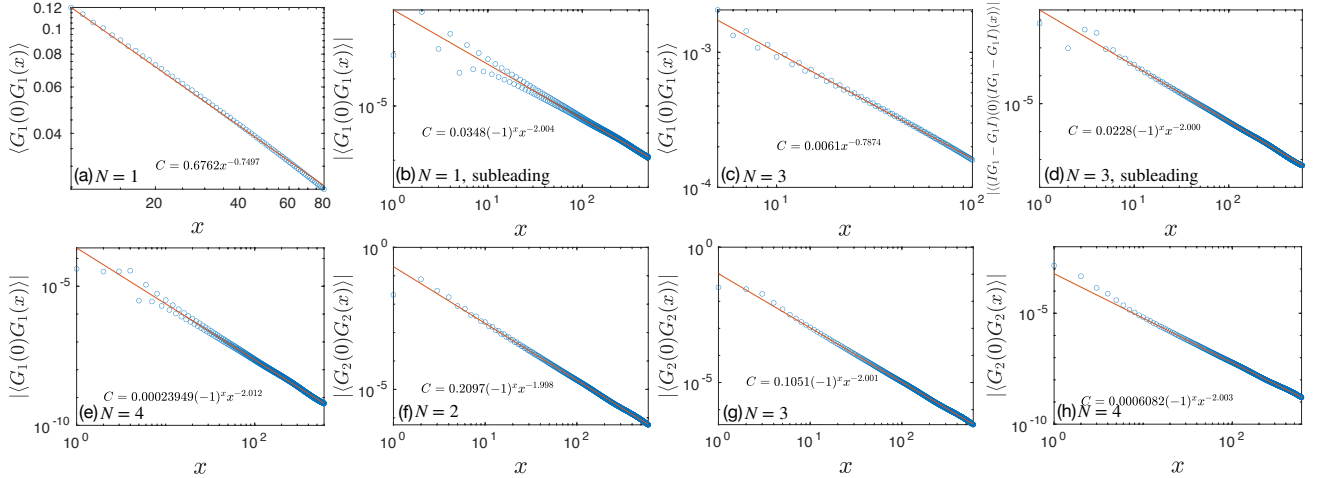


FIG. S5. The absolute value of the correlation function $\langle G_1(0)G_1(x) \rangle$ and $\langle G_2(0)G_2(x) \rangle$ measured with MPS of bond dimension $\chi = 240$, where G_1 and G_2 are the optimal solution for MPS of bond dimension $\chi = 400$. The subleading part of the correlation function of the N -site operator G is obtained by measuring the correlation function of $G \otimes I - I \otimes G$, and therefore the subleading part of the correlation function of the 1-site G_1 is equivalent to the correlation function of the 2-site G_1 .

In Fig. S5 we show the correlation function of G_1 and G_2 for different N and confirm that their scaling dimension is pinned at one. We can see that

$$\langle G_1(0)G_1(r) \rangle \sim c_1 r^{-g/2} + c_2 (-1)^r r^{-2}, \quad \langle G_2(0)G_2(r) \rangle \sim (-1)^r r^{-2}, \quad (\text{S58})$$

where $g \approx 1.5$ is the Luttinger parameter [8]. Notice that $\langle G_1(0)G_1(r) \rangle \sim (-1)^r r^{-2}$ for even N because of the cancellation of the non-staggered part due to terms like $G \otimes I - I \otimes G$, where G is a $N-1$ -site operator, as listed in Table III. This cancellation can be explained as follows. If $\langle G(0)G(r) \rangle \sim c_1 r^{-1} + c_2 (-1)^r r^{-2}$, then

$$\begin{aligned}
& \langle (G \otimes I - I \otimes G)(0)(G \otimes I - I \otimes G)(r) \rangle \\
&= \langle G(0)G(r) \rangle - \langle G(0)G(r+1) \rangle - \langle G(1)G(r) \rangle + \langle G(1)G(r+1) \rangle \\
&= 2[c_1 r^{-1} + c_2 (-1)^r r^{-2}] - c_1 (r+1)^{-1} - c_2 (-1)^{r+1} (r+1)^{-2} - c_1 (r-1)^{-1} - c_2 (-1)^{r-1} (r-1)^{-2} \\
&\sim 4c_2 (-1)^r r^{-2}.
\end{aligned} \tag{S59}$$

Here we also provide results of the eigenvalues of the optimization problem at $p=0$ from $N=1$ to $N=4$. None of them have scaling dimension one, and thus none of them are emergent conserved currents.

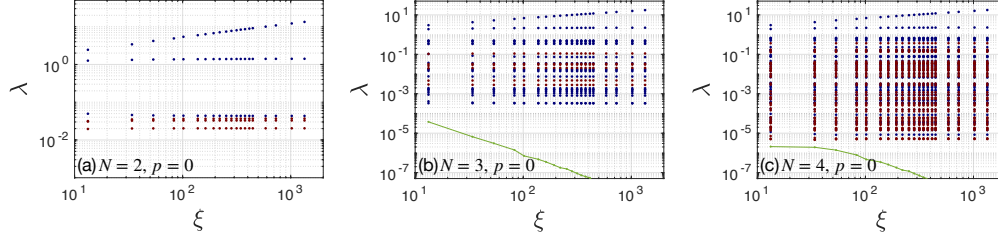


FIG. S6. Log-log plot of the non-trivial eigenvalue spectrum of \mathcal{F} (with time reversal and parity symmetry imposed) versus the correlation length ξ at $p=0$ for the Jiang-Motrunich model at $J_z = 1.4645$. The G 's associated with the blue (red) dots are parity even (odd) and time reversal odd (even). The green curve is the Hamiltonian.

In Table III we list the optimal G 's we obtained with MPS of bond dimension $\chi = 400$ from $N=1$ to $N=4$ for the Jiang-Motrunich model.

p	N	\mathcal{P}	\mathcal{T}	G
0	1			—
	2			—
	3	+	+	$-(IXX + XXI) - 1.4645(IZZ + ZZI) + (XIX + ZIZ)$
π	1	+	-	Z
	2	-	+	$XY + YX$
		+	-	$ZI - IZ$
	3	-	+	$0.154265[(XY + YX)I - I(XY + YX)] + 0.122085(XIY - YIX)$
		+	-	$0.182771(-ZII + IZI - IIZ)$
				$+0.088579ZZZ + 0.054162(YYZ + ZYY) + 0.048393(XXZ + ZXX) + 0.022477XZX - 0.076692YZY$
				$II(XY + YX) - I(XY + YX)I + (XY + YX)II$
				$+0.775400(-IXIY + IYIX + XIYI - YIXI) + 0.178269(XIIY + YIIX)$
				$+0.957965(XZZY + YZZX) - 0.758349(XXXY + YXXX) + 0.517924(XYYY + YYYX)$
				$-0.397084(XZYX + ZYZX)$
	4	-	+	$+0.334832(YZXX + ZXZY) + 0.333265(XYZZ + ZZYX)$
				$+0.332877(XXYX + XYXX) + 0.306209(YXZZ + ZZXY)$
				$-0.222842(YXYX + YYXY) + 0.188941(ZXYZ + ZYXZ)$
				$0.015692(-III Z + IIZI - IZII + ZIII)$
				$-0.094125(XIZX - XZIX) + 0.072197(XXIZ - ZIXX)$
				$-0.064930(XIXZ - ZXIX) + 0.058821(ZIZZ - ZZIZ)$
				$+0.048485(IXXZ + IZXX - XXZI - ZXXI)$
				$+0.043120(IXZX - XZXI) + 0.032214(YIZY - YZiy) - 0.030060(IZZZ - ZZZI)$
				$+0.012363(IYYZ - ZYYI + IZYY - YYZI) + 0.011590(YYIZ - ZIYY)$
				$-0.005822(YIYZ - ZYiy) + 0.005798(IYZY - YZYI)$

TABLE III. Optimal lattice operator approximation of the emergent conserved currents in the Jiang-Motrunich model at $J_z = 1.4645$ up to $N=4$ with $\chi = 400$. + (-) means parity \mathcal{P} or time reversal \mathcal{T} even (odd).